Bulletin of the Geological Survey of Japan, vol. 68 (3), p. 87–110, 2017

Article

Influence of different sedimentary environments on multi-elemental marine geochemical maps of the Pacific Ocean and Sea of Japan, Tohoku region

Atsuyuki Ohta[1,*], Noboru Imai[1], Yoshiko Tachibana[1], Ken Ikehara[1], Hajime Katayama[1] and Takeshi Nakajima[2]

Atsuyuki Ohta, Noboru Imai, Yoshiko Tachibana, Ken Ikehara, Hajime Katayama and Takeshi Nakajima (2017) Influence of different sedimentary environments on multi-elemental marine geochemical maps of the Pacific Ocean and Sea of Japan, Tohoku region. *Bull. Geol. Surv. Japan*, vol. 68 (3), p. 87–110, 9 figs, 5 tables.

Abstract: The authors present comprehensive terrestrial and marine geochemical maps of the Tohoku region and examine how marine sedimentary environments affect the spatial distribution of elemental concentrations. Marine sediments from the Sea of Japan are relatively enriched in elements abundant in felsic igneous rocks such as K_2O, Ba, and REEs. These elements are highly enriched in sediments around submarine topographic highs, and are products of the denudation of Neogene sedimentary rocks associated with dacitic tuff and barite nodules. The silt and clay in deep basins are abundant in elements such as MnO, Cd, and Pb because of early diagenetic processes. Silty sediments on the continental shelf are supplied by large rivers; however, their geochemical features are influenced not by the adjacent terrestrial materials but simply by the effects of grain size. The sandy sediments that extensively cover the seafloor of the Pacific Ocean in the study area were sampled from depths below wave base (100–1,000 m). Their chemical compositions are homogenous and similar to those of stream sediments that originate from mafic volcanic rocks. Therefore, they are inferred to have been deposited as relict sediments under the influence of Quaternary mafic volcanic activity that have been transported from the shelf to the deep sea by gravity currents. Although 81% of the total terrestrial sediment yield is discharged into the Sea of Japan, the spatial distributions of elemental concentrations are not always continuous between land and sea. Similar findings are recognized for the Pacific Ocean side. Notably, coarse sands distributed offshore from Kamaishi are enriched in elements abundant in sedimentary rocks of the accretionary complexes and granitic rocks that crop out in adjacent terrestrial areas. Because the river system in this region is small and has low sediment yields, these coarse sands may have been produced via coastal erosion or denudation of parent rocks during past regression and transgression.

Keywords: geochemical mapping, sedimentary environment, stream sediment, marine sediment, Tohoku region, Pacific Ocean, Sea of Japan

1. Introduction

The Geological Survey of Japan has conducted research on the spatial distributions of elements across the earth's surface ("geochemical mapping") to elucidate the natural background amounts of these elements (Imai *et al*., 2004, 2010). A geochemical map provides fundamental geo-information about the elemental cycle in the upper crust, and can be applied for environmental assessment and mineralogical exploration (e.g., Webb *et al*., 1978; Howarth and Thornton, 1983; Weaver *et al*., 1983). Recently, cross-boundary and sub-continental-scale geochemical mapping has been an active area of research (e.g., Reimann *et al*., 2003; Salminen *et al*., 2005). We conducted the first comprehensive survey of elemental distributions in both terrestrial and marine environments because Japan is surrounded by seas. Previously, we have established a procedure for multi-elemental analysis of geochemical mapping data sets (Ohta *et al*., 2007) and proposed its application in investigating particle

[1] AIST, Geological Survey of Japan, Research Institute of Geology and Geoinformation

[2] AIST, Geological Survey of Japan, Research Institute for Geo-Resources and Environment

[*] Corresponding author: A. Ohta,Central 7,1-1-1 Higashi, Tsukuba, Ibaraki 305-8567, Japan. Email: a.ohta@aist.go.jp

transportation processes from land to sea and within marine environments (Ohta and Imai, 2011), as well in provenance study of marine sediments (Ohta *et al*., 2013).

In this paper, we describe terrestrial and marine geochemical maps for the Tohoku region of northern Japan. The geochemistry of marine sediments in the northeastern Sea of Japan have been studied in detail by Terashima and Katayama (1993), Terashima *et al*. (1995a, b), and Imai *et al*. (1997) as a pilot study for regional marine geochemical mapping. They discussed the geochemical features of heavy elements such as Cr, Mn, Fe, Ni, Cu, Zn, Hg, and Pb in marine sediments, but did not sufficiently examine the relationships between stream and marine sediments. The Pacific Ocean adjacent to the Tohoku region is located in a subduction zone characterized by the Japan Trench, and subduction earthquakes have occurred in this region. In particular, the major earthquake in 2011 caused a catastrophic disaster in the northern Japan. Therefore, scientific interest has been focused primarily on tsunami sediments in the coastal frontal zone and on the deep marine sediments of the Japan Trench. Sedimentation on the continental shelf and slope in the Pacific Ocean near the Tohoku region has been investigated relatively little (Iijima and Kagami, 1961; Nakajima, 1973). Furthermore, the marine environment around the Tohoku region differs considerably between the Sea of Japan and the Pacific Ocean. The Tohoku region is therefore suitable for studying the effects of different sedimentary environments on elemental concentrations. The purpose of this study is to examine how various depositional environments affect the spatial distribution patterns of elements in marine sediments.

2. Study area

2. 1 Riverine system

Figure 1 displays a schematic map of the study area with elevation and water depth. The Ou Mountain Range, with elevations ranging from 1,000 to 2,000 m, extends north–south in the northern part of the Tohoku region and separates the study area into the Pacific Ocean side and the Sea of Japan side. Sixteen major river systems exist in the study area. The potential sediment yields of these rivers are listed in Table 1 (Akimoto *et al*., 2009); 81% of the

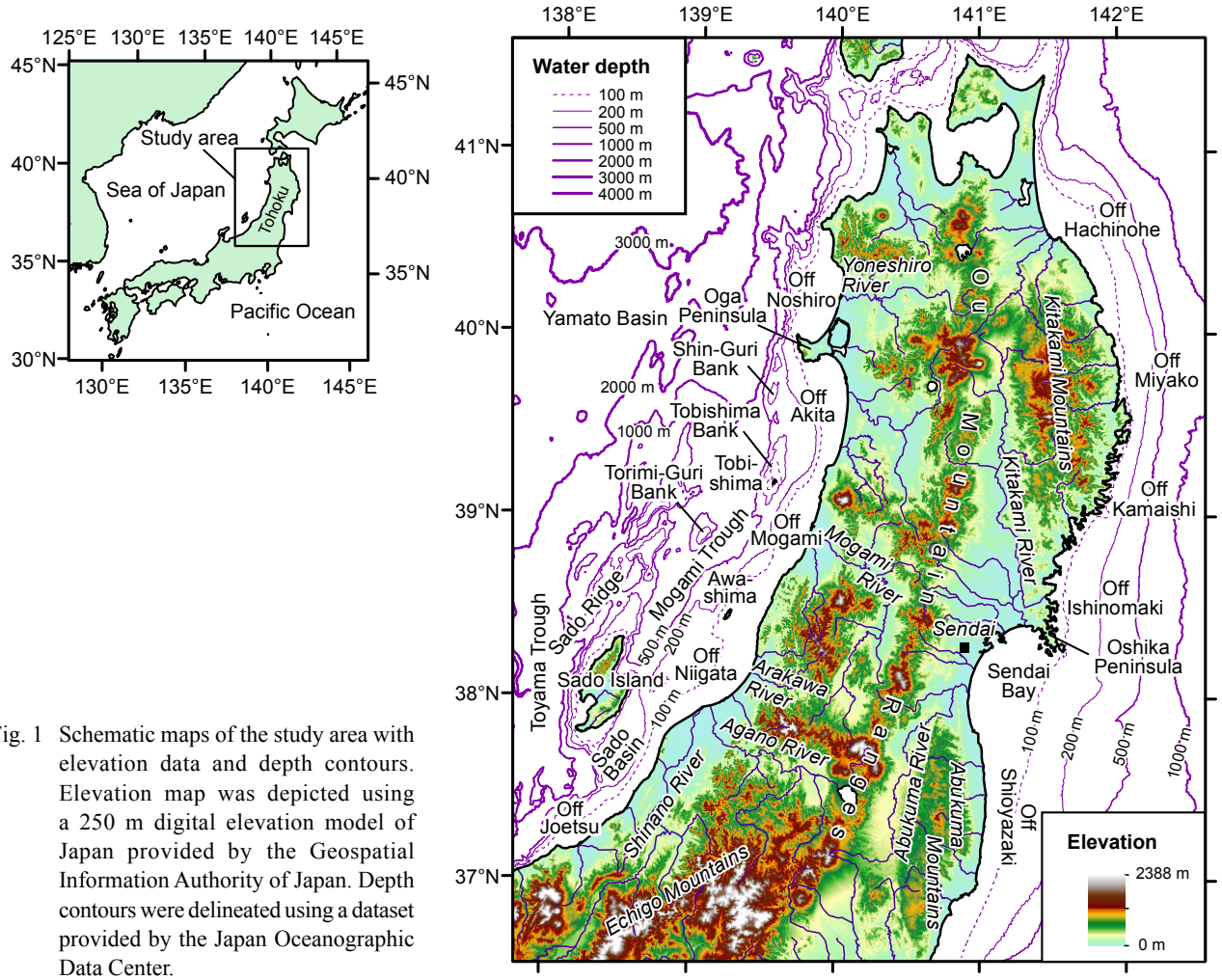

Fig. 1 Schematic maps of the study area with elevation data and depth contours. Elevation map was depicted using a 250 m digital elevation model of Japan provided by the Geospatial Information Authority of Japan. Depth contours were delineated using a dataset provided by the Japan Oceanographic Data Center.

Table 1 Sediment yield and river water discharge data for each river system of the study area.

River system	Average rate of sediment yield[a]	Drainage basin area[b]	Sediment yield	Water discharge in 2000[b]	Discharged area	Relative rate to total sediment yield
	$m^3/km^2/year$	km^2	$m^3/year$ ($\times10^3$)	$m^3/year$ ($\times10^6$)		
Iwaki	121	1740	211	2789	Sea of Japan	2.1%
Yoneshiro	180	2109	380	3446	Sea of Japan	3.8%
Omono	183	4035	738	8735	Sea of Japan	7.4%
Koyoshi	170	937	159	2156	Sea of Japan	1.6%
Mogami	217	6271	1361	12503	Sea of Japan	14%
Aka	248	552	137	2390	Sea of Japan	1.4%
Ara	313	905	283	640	Sea of Japan	2.8%
Agano	249	6997	1742	13188	Sea of Japan	17%
Shinano	298	9719	2896	15247	Sea of Japan	29%
Seki	324	703	228	1651	Sea of Japan	2.3%
Takase	n.d.	344	46[c]	559	Pacific Ocean	0.5%
Mabuchi	135	1751	236	1925	Pacific Ocean	2.4%
Kitakami	149	7869	1173	11688	Pacific Ocean (Sendai Bay)	12%
Naruse	106	551	58	893	Pacific Ocean (Sendai Bay)	0.6%
Natori	146	424	62	517	Pacific Ocean (Sendai Bay)	0.6%
Abukuma	136	1865	254	2127	Pacific Ocean (Sendai Bay)	2.5%

[a] Akimoto *et al* . (2009) Proceedings of Hydraulic Engineering 53, 655-660.

[b] Ministry of Land, Infrastructure, Transport and Tourism (http://www.mlit.go.jp/river/toukei_chousa/, accessed in Nov. 19, 2015)

[c] Average rate of sediment yield of Takase River is assumed to be the same as that of Mabuchi River.

total terrestrial sediment yield is discharged into the Sea of Japan. The Shinano and Agano Rivers are the largest of this region; these rivers have high sediment yields to the coast of Niigata: 29% and 17%, respectively, of the total sediment discharge of this region. In contrast, the rivers flowing to the Pacific Ocean supply only 19% of the total sediment yield of the study area. Most of these rivers flow through the Sendai Plain to Sendai Bay area.

2. 2 Geology of the terrestrial area

Figure 2 shows a geological map of northern Japan that has been simplified from the Geological Map of Japan 1:1,000,000 scale (Geological Survey of Japan, 1992). Jurassic sedimentary rocks of accretionary complexes crop out in the Kitakami Mountains, which are called the Kitakami Belt. These strata are associated with Permian–Carboniferous limestone and basalt, Carboniferous–Jurassic chert, and ultramafic rocks. Cretaceous granites were intruded into the southern Kitakami, Abukuma, and Asahi Mountains. Miocene–Pliocene granite is found in the Echigo Mountains. Cretaceous metamorphic rocks associated with Cretaceous granitic rocks are distributed in the regions of the Kitakami, Abukuma and Asahi Mountains. Mafic and felsic volcanic rocks associated with debris and pyroclastic rocks erupted mainly during the Neogene and Quaternary. A third part of the study area is covered by these volcanic rocks. Quaternary mafic volcanic and pyroclastic rocks and debris are distributed along a line to form the Ou Mountains. Neogene and Quaternary sediments are the most widely distributed units in the area; they are exposed across 40% of the study area and form wide plains in the Tohoku region. Carboniferous, Cretaceous, Jurassic, and Paleogene sedimentary rocks are distributed in the southern Kitakami Mountains.

There are many economically important deposits mined in the study area. Kuroko-type deposits are found in the Kosaka and Hanaoka mines, which bear Cu, Pb, Zn, Au, and Ag ores. Most of these deposits occur in the watershed of the Yoneshiro River. The Oppu, Hosokura and Ohizumi mines are hydrothermal vein-type and bear Zn, Pb, and Cu. In particular, the Au mine on Sado Island mines the largest known hydrothermal vein deposit in Japan. Skarn-type deposits, like that of the Kamaishi mine that bears Fe, Cu and W, are found in granitic intrusions in the regions of the Kitakami and Abukuma Mountains.

2. 3 Coastal areas and marine geology

Figure 1 shows that the seafloor topography of the Sea of Japan is uneven, with a narrow continental shelf, submarine ridges, isolated seamounts, and deep basins. The Sado Basin, Mogami Trough, Toyama Trough, and Yamato Basin are all deep-sea basins of this sea. The Sado Ridge, Shin-Guri Bank, Tobishima Bank, and Torimi-Guri Bank are submarine topographic highs. In contrast, a gentle slope is found in the Pacific Ocean near Tohoku.

Figure 2 also shows marine geology based on the Geological Map of Japan 1:1,000,000 scale (Honza *et al*., 1978; Tamaki *et al*., 1981) and marine faults below the Sea of Japan reported by Okamura (2013). Numerous active faults lie in a NNE–SSW orientation in the Sea of Japan, where many large earthquakes have occurred (Okamura, 2010). Basement rocks in the Sea of Japan are thought to consist of Cretaceous granitic intrusions, Jurassic accretionary complexes, and Miocene to Pliocene

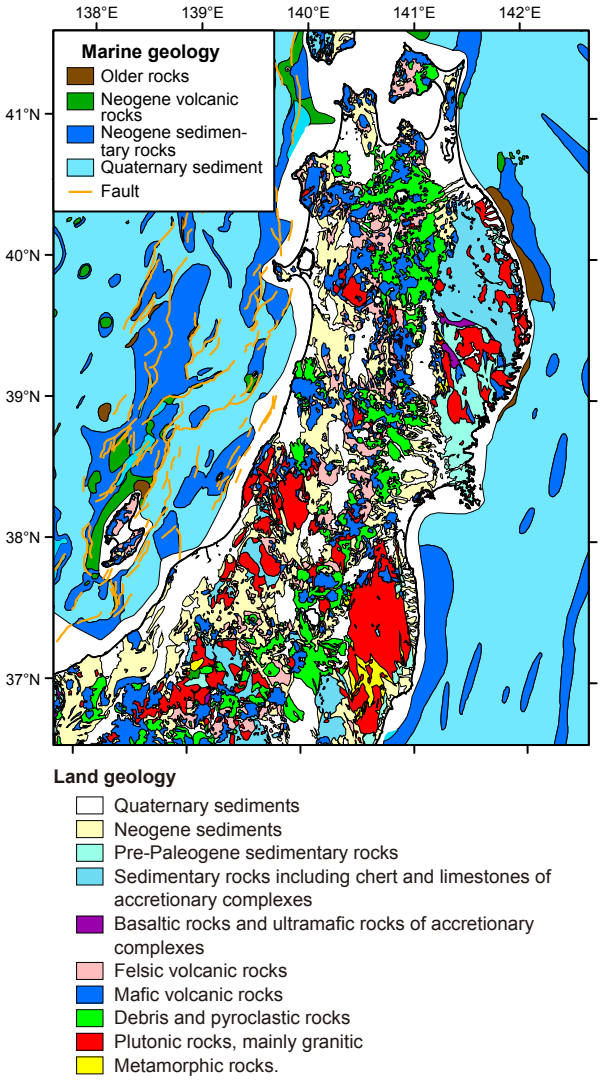

Fig. 2 Geological map of the Tohoku region of Japan, 1:1,000,000 scale (Geological Survey of Japan, 1992; Honza *et al*., 1978; Okamura, 2013; Tamaki *et al*., 1981). The older rocks of the marine geology are Paleogene, Cretaceous, and Jurassic in age (see the text).

siltstone–mudstone (Okamura *et al*., 1995a). These basement rocks form exposed topographic highs. The continental shelf and deep basins are covered with thick deposits of modern sediments.

In the Pacific Ocean, Miocene volcanic rocks are distributed on the continental shelf offshore from Hachinohe (Tamaki, 1978). Basement rocks of the continental shelf off of Hachinohe and Kamaishi are composed of Cretaceous to Paleogene sedimentary rocks (Tamaki, 1978), and offshore basement rocks are Miocene–Pleistocene sedimentary rocks containing volcanic materials (Okamura and Tanahashi, 1983). Basement rocks of the continental shelf off of Shioyazaki are composed of Pliocene sedimentary rocks. Quaternary sediments overlie these basement rocks (Arita and Kinoshita, 1978, 1984). In contrast to the Sea of Japan, there are few active faults below this region of the Pacific Ocean.

3. Materials

Figure 3 shows the sampling locations of stream and marine sediments. A total of 798 stream sediment samples for combined geochemical mapping were collected from the Tohoku region during 1999–2002 (Imai *et al*., 2004). The mean sampling density is one sample per 100–120 km^2. Stream sediments were air dried and sieved with an 83 mesh (180 μm) screen. In addition, magnetic minerals were removed from the samples using a hand magnet to minimize the effect of magnetic mineral accumulation (Imai *et al*., 2004). Imai (1987) reported that fine fractions such as these have similar elemental compositions to bulk sediment samples.

First, 392 marine sediment samples were collected from the Pacific Ocean during Cruises GH81-1, GH81-2, and GH81-3 in 1981 (Arita and Kinoshita, 1978, 1984; Nishimura and Saito, 2016). An additional 405 marine sediments were collected from the Sea of Japan during Cruise GH90 in 1990 and Cruise GH91 in 1991 (Ikehara *et al*., 1994a, b; Katayama *et al*., 1994; Nakajima *et al*., 1995). Sixty additional samples were collected from the northern Tohoku region during Cruises GC06-01 and GC06-02 Cruises in 2006. These marine sediment samples were collected using a grab sampler. The uppermost 3 cm of collected sediments was separated, air dried, ground, and retained for analysis. Some samples were predominantly composed of rock fragments and gravels. In such case, we collected the sandy matrix materials.

To characterize marine sediment textures, each sampling location was assigned its own symbol according to grain size; they are classified into four categories based on the median particle diameter (φ-scale) of surface sediments. *Coarse sediments* comprise rock fragments, gravels, and very coarse, coarse and medium sands ($\varphi \leq 2$); *fine sand* comprises fine and very fine sands ($2 < \varphi \leq 4$); and *silt* and *clay* consist of particles with diameters of $4 < \varphi \leq 8$ and $\varphi \geq 8$, respectively. An additional 226 samples that were not measured for median particle diameter are classified based on textures identified through visual inspection conducted onboard the research vessel. Figure 3 shows that samples collected from the Pacific Ocean are composed mainly of sandy sediments. Coarse sands are predominantly distributed on the continental shelf off of Hachinohe and in the southern part of Sendai Bay. Silt is deposited in Sendai Bay, in the region offshore from Ishinomaki and Shioyazaki, and on the deep continental slope (>500 m). In contrast, more than half of the samples from the Sea of Japan are composed of clay. Silt and clay samples were collected from deep-sea basins, particularly from the continental shelf off of Niigata and Akita. Sandy

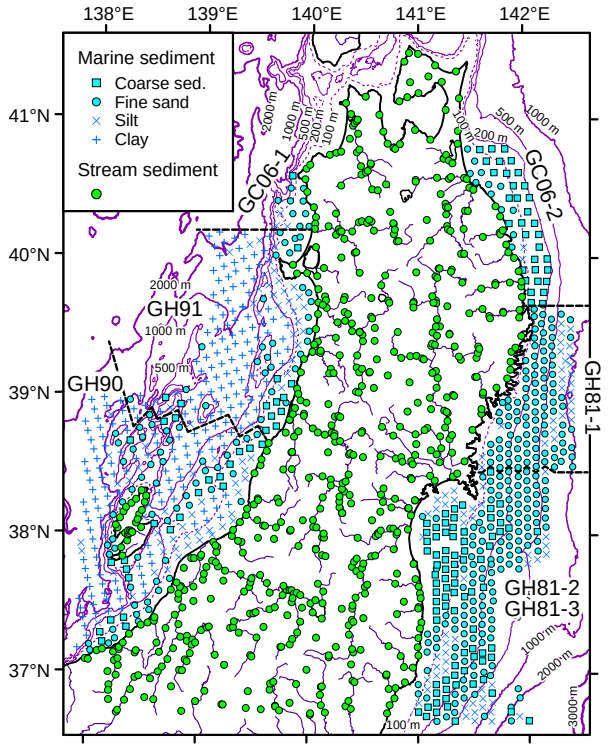

Fig. 3 Sampling locations of stream and marine sediments.

sediments from the Sea of Japan were collected from the continental shelf and submarine topographic highs.

4. Methodology

The analytical methods and quality control of the geochemical data have been described by Imai (1990), Ujiie-Mikoshiba *et al*. (2006), and Ohta *et al*. (2013). Each sample was digested for 2 h using a mixed solution of HF, HNO_3 and $HClO_4$ at 120°C. The degraded product was evaporated to dryness at 200°C; the residue was then dissolved in 100 mL of 0.35 M HNO_3 solution. The concentrations of 53 elements were determined using ICP-AES (major elements, V, Sr, and Ba) and ICP-MS (minor elements) (Imai *et al*., 2004, 2010). Analyses of the As contents of all samples and Hg content of stream sediment and marine sediment samples from the Sea of Japan were subcontracted to ALS Chemex in Vancouver, B.C. Levels of Hg in marine sediments from the Pacific Ocean were determined using an atomic absorption spectrometer. A portion of the geochemical data reported in pilot studies (e.g., the Hg data of Terashima *et al*., 1995a) was used for nationwide marine geochemical mapping. In this study, the V, Co, and Zn data of Imai *et al*. (1997) and Terashima *et al*. (1995b) were also used for the analysis. Table 2 summarizes of the analytical results obtained for marine and stream sediments. Data for Na_2O content in marine sediments are only advisory because marine sediments were not desalinated. Zr and Hf data are excluded because of unsatisfactory digestion of minerals that host Zr and Hf using the HF, HNO_3 and $HClO_4$ solution.

The spatial distribution patterns of elements in both terrestrial and marine environments were determined using geographic information system (GIS) software (ArcGIS 10.3; Environmental Systems Research Institute, Inc.) after Ohta and Imai (2011). Class selection of elemental concentrations was conducted separately for terrestrial and marine environments because these environments differ in chemical and mineralogical compositions, particle size, and origins (Ohta and Imai, 2011). Percentiles are used for class selections for the elemental concentration intervals used in maps, i.e., the 5th, 10th, 25th, 50th, 75th, 90th, and 95th percentiles (Reimann, 2005). The spatial distribution patterns of mud (silt and clay) content by weight % in marine environments were also determined using this method. Mud contents were not recorded from GH81-2, GH81-3, GC06-01, and CG06-02; therefore, the mud contents of marine sediments off of Hachinohe and Miyako reported by Arita and Kinoshita (1978) were used to create the mud distribution map. Geochemical maps of mud content and 15 elements (Al_2O_3, K_2O, CaO, MnO, Fe_2O_3, Cr, Cu, As, Cd, Cs, Ba, La, Yb, Pb, and U) are shown in Fig. 4.

5. Results

5. 1 Spatial distributions of elements in terrestrial areas

Sampling locations and their geography, geology and geochemical backgrounds have previously been reported by Ohta *et al*. (2011) and Ujiie-Mikoshiba *et al*. (2006). Therefore, we simply summarize these features herein. Mafic volcanic rocks are associated with elevated MgO, Al_2O_3, P_2O_5, CaO, Sc, TiO_2, V, MnO, Fe_2O_3, Co, Cu, Zn, and Sr concentrations in stream sediments, but with lower Li, Be, Na_2O, K_2O, Rb, Nb, Sn, Cs, Ba, Ta, Tl, Th, and U concentrations. Pyroclastic rocks and debris exert an effect similar to that of mafic volcanic rocks. For example, K_2O and Ba concentrations are low in the Ou Mountains covered by mafic volcanic rocks and pyroclastic rocks, but these concentrations are rather high in the western Ou Mountains where mafic and felsic volcanic rocks and Neogene sedimentary rocks are distributed. Be, Na_2O, K_2O, Ga, Rb, Nb, Sn, rare earth elements (REEs: Y and lanthanides), Ta, Tl, Th, and U are highly enriched in stream sediments collected from areas underlain by granitic rocks; especially high concentration of these elements are found in the Asahi and Echigo Mountains. Stream sediments collected from the northern Kitakami Mountains, which are covered by accretionary complexes, are abundant in Li, Be, K_2O, Rb, Cs, light REEs (La, Ce, Pr, Nd, and Sm), and Th. Ultramafic rock especially elevates MgO, TiO_2, Cr, MnO, Co, Ni and Cu concentrations in stream sediments; however, distribution of these elements is highly restricted in the southern Kitakami Mountains.

Table 2 Summary of the geochemistry of marine and stream sediments for the Tohoku region, Japan.

		Marine sediment (*N=857*)					Stream sediment (*N=655*)				
Element	Unit	Min	Median	Mean	Max	MAD	Min	Median	Mean	Max	MAD
Na_2O	wt%	1.08	3.12	3.34	5.62	0.46	0.61	2.19	2.19	3.87	0.32
MgO	wt%	0.67	3.28	3.34	5.99	0.68	0.71	2.75	2.99	8.85	0.70
Al_2O_3	wt%	1.05	8.73	8.74	16.8	0.98	5.55	11.2	11.1	19.4	1.59
P_2O_5	wt%	0.036	0.115	0.126	0.447	0.023	0.027	0.118	0.137	3.46	0.031
K_2O	wt%	0.215	1.63	1.62	2.91	0.26	0.271	1.47	1.51	3.06	0.32
CaO	wt%	0.631	2.77	3.12	39.6	1.45	0.262	2.67	2.83	8.55	0.92
TiO_2	wt%	0.033	0.461	0.465	1.43	0.052	0.175	0.732	0.813	4.26	0.168
MnO	wt%	0.017	0.075	0.139	2.19	0.020	0.030	0.128	0.135	0.628	0.030
Fe_2O_3	wt%	0.85	4.66	5.08	18.4	0.78	2.11	6.29	6.51	26.1	1.38
Li	mg/kg	5.70	26.5	28.0	62.1	9.25	5.78	20.9	22.0	67.9	5.27
Be	mg/kg	0.16	1.13	1.16	3.85	0.21	0.19	1.14	1.21	5.49	0.23
Sc	mg/kg	1.80	10.8	11.2	38.0	2.54	4.23	16.0	16.9	62.1	4.74
V	mg/kg	8.0	89	87	219	14	29	125	134	383	37
Cr	mg/kg	7.4	47.9	48.0	199	11.2	6.4	46.3	60.1	605	16.4
Co	mg/kg	1.0	9.0	9.4	39	1.6	3.18	14.4	15.4	43.5	4.21
Ni	mg/kg	3.98	17.3	21.2	136	6.27	2.54	16.2	22.5	277	5.99
Cu	mg/kg	2.97	14.5	17.8	57.9	6.84	3.49	24.1	33.0	523	8.42
Zn	mg/kg	10	87	87	221	15	52.0	116	145	5382	26
Ga	mg/kg	1.87	13.0	12.8	18.4	0.97	7.92	16.0	16.1	22.4	0.99
As	mg/kg	1.0	8.2	11	141	3.9	1.0	9.0	14	234	4.0
Rb	mg/kg	4.56	46.1	46.7	120	11.7	5.29	45.0	52.0	242	15.5
Sr	mg/kg	70	168	189	2089	45	51	156	163	426	38
Y	mg/kg	5.56	13.4	13.5	22.2	1.96	6.44	18.5	19.3	48.6	3.40
Nb	mg/kg	0.73	5.13	4.88	9.32	0.96	0.92	6.20	6.77	25.0	1.41
Mo	mg/kg	0.29	0.99	1.68	38.2	0.36	0.17	1.37	1.73	24.0	0.46
Cd	mg/kg	0.015	0.079	0.105	0.79	0.027	0.026	0.16	0.31	19.7	0.064
Sn	mg/kg	0.29	1.33	1.51	3.30	0.47	0.47	1.79	2.57	168	0.48
Sb	mg/kg	0.045	0.51	0.62	2.10	0.16	0.066	0.60	1.01	123	0.20
Cs	mg/kg	0.24	2.41	2.83	7.40	1.02	0.63	2.45	2.92	12.6	0.82
Ba	mg/kg	49	311	364	12500	51	142	389	390	1337	63
La	mg/kg	3.76	12.2	12.1	42.4	2.13	2.16	14.2	15.8	135	3.65
Ce	mg/kg	6.99	20.5	22.4	104	3.41	4.48	26.2	30.0	268	6.51
Pr	mg/kg	0.88	2.95	2.98	10.7	0.47	0.62	3.48	3.84	28.4	0.79
Nd	mg/kg	3.57	12.0	12.2	41.9	1.66	3.02	14.4	15.7	103	2.92
Sm	mg/kg	0.82	2.63	2.65	8.04	0.30	0.94	3.19	3.44	17.9	0.53
Eu	mg/kg	0.27	0.68	0.71	1.73	0.08	0.31	0.85	0.87	1.78	0.11
Gd	mg/kg	0.78	2.53	2.54	6.65	0.26	1.07	3.18	3.36	13.1	0.50
Tb	mg/kg	0.16	0.45	0.45	1.00	0.05	0.25	0.57	0.60	1.82	0.09
Dy	mg/kg	0.90	2.30	2.32	4.45	0.26	1.19	3.06	3.17	8.14	0.52
Ho	mg/kg	0.19	0.45	0.45	0.77	0.06	0.21	0.61	0.63	1.60	0.11
Er	mg/kg	0.50	1.33	1.34	2.15	0.18	0.60	1.83	1.89	4.72	0.32
Tm	mg/kg	0.077	0.21	0.21	0.34	0.03	0.091	0.29	0.31	0.74	0.05
Yb	mg/kg	0.47	1.33	1.34	2.13	0.19	0.55	1.85	1.92	4.75	0.32
Lu	mg/kg	0.067	0.20	0.20	0.33	0.03	0.078	0.27	0.29	0.68	0.05
Ta	mg/kg	0.004	0.41	0.40	0.74	0.10	0.015	0.50	0.56	2.25	0.13
Hg	mg/kg	0.0005	0.045	0.071	1.19	0.023	0.001	0.030	0.086	18	0.020
Tl	mg/kg	0.056	0.36	0.36	0.75	0.10	0.09	0.43	0.48	6.54	0.14
Pb	mg/kg	4.90	21.2	26.6	83.6	9.29	4.82	20.2	37.9	7594	6.43
Bi	mg/kg	0.015	0.26	0.37	1.45	0.16	0.026	0.21	0.50	87.0	0.08
Th	mg/kg	0.67	3.74	3.68	14.8	0.87	0.64	4.25	7.10	363	1.69
U	mg/kg	0.25	0.92	0.96	2.91	0.22	0.16	1.19	1.63	86.2	0.39

Minimum (Min), maximum (Max), and median absolute deviation (MAD).

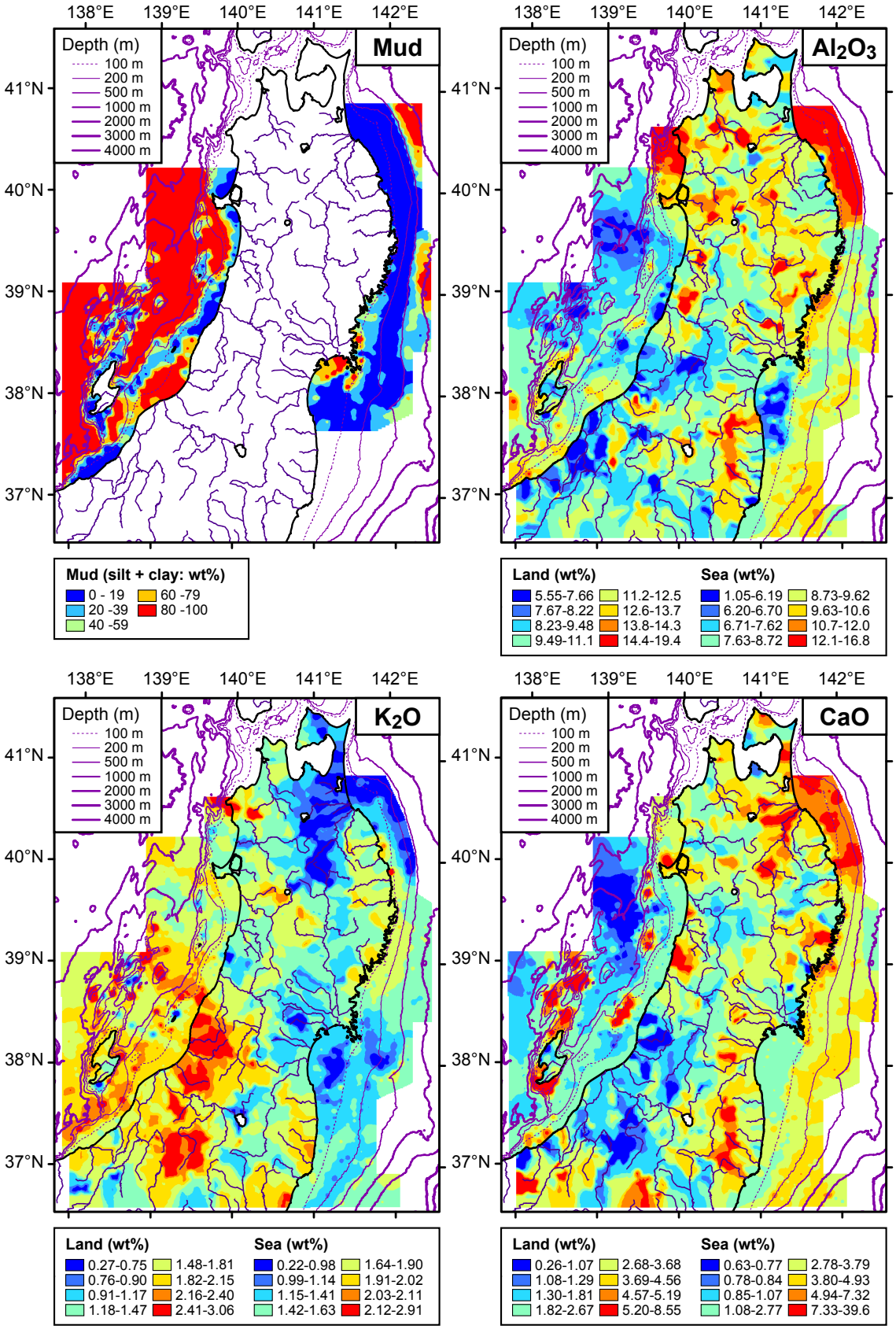

Fig. 4 Spatial distributions of mud content in marine areas and of elemental concentrations in terrestrial and marine areas for Al_2O_3, CaO, K_2O, T-Fe_2O_3, MnO, Cr, Cu, As, Cd, Cs, Ba, La, Yb, Pb, and U. Star, cross, circle, and diamond, symbols indicate major metalliferous deposits.

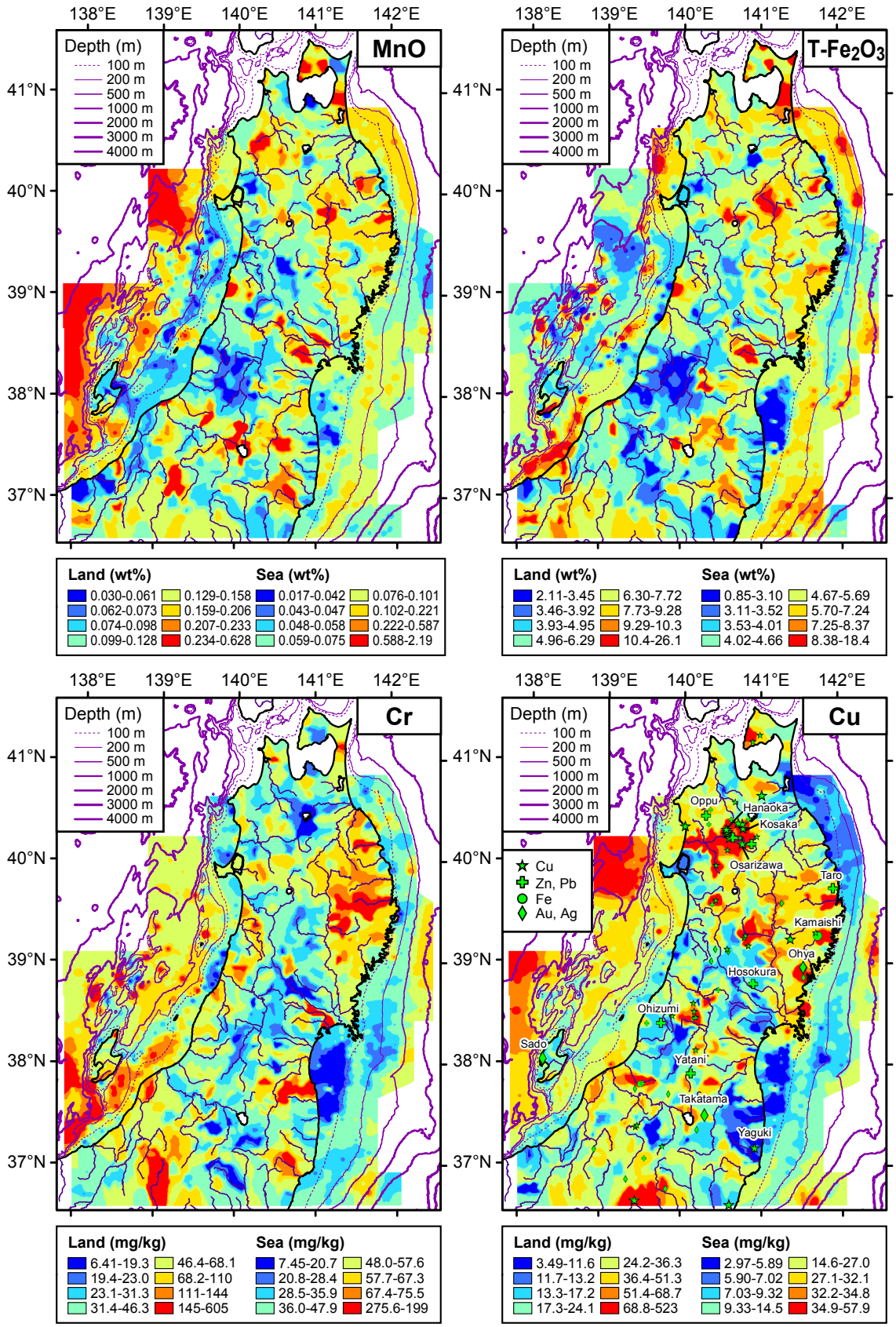

Fig. 4 Continued.

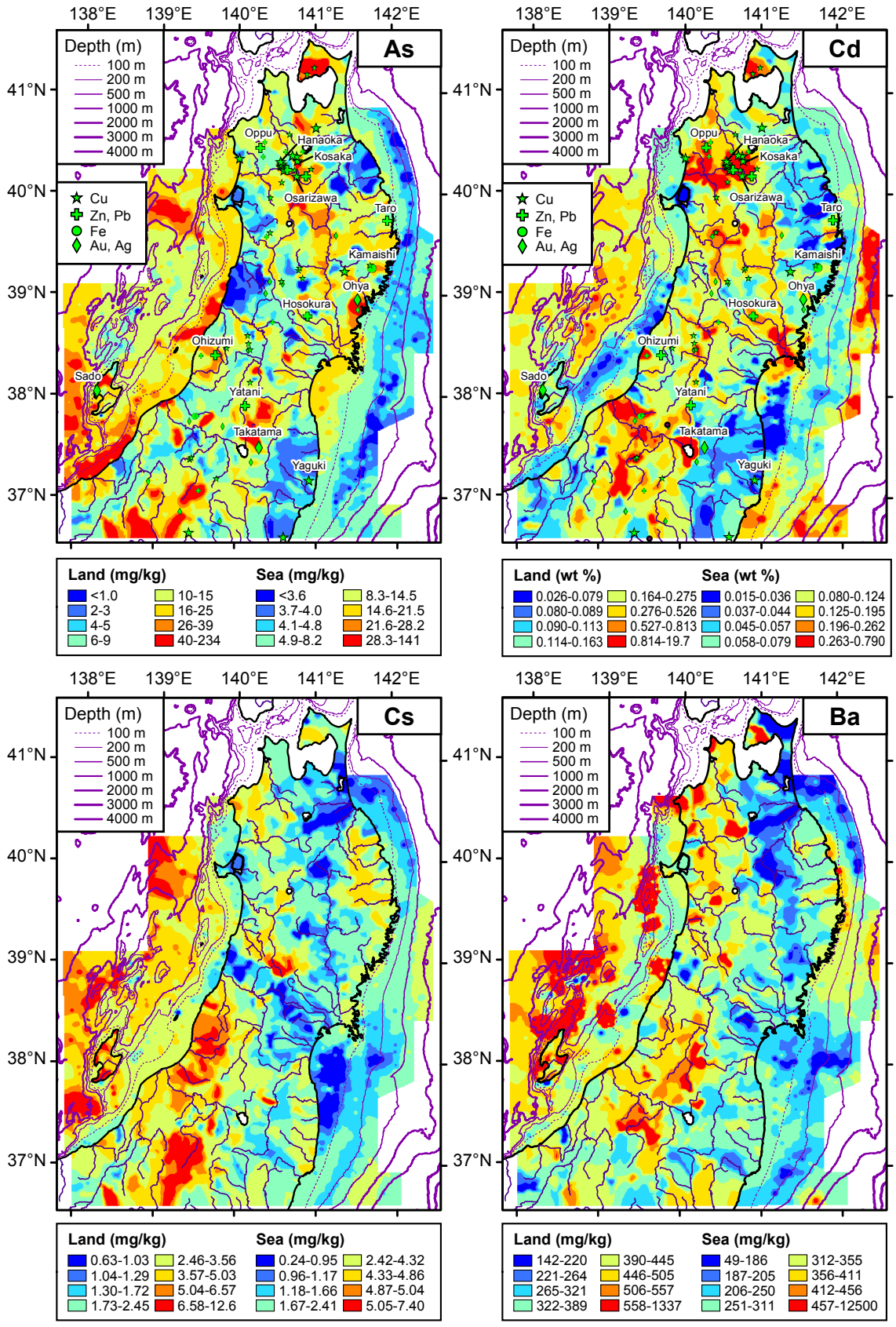

Fig. 4 Continued.

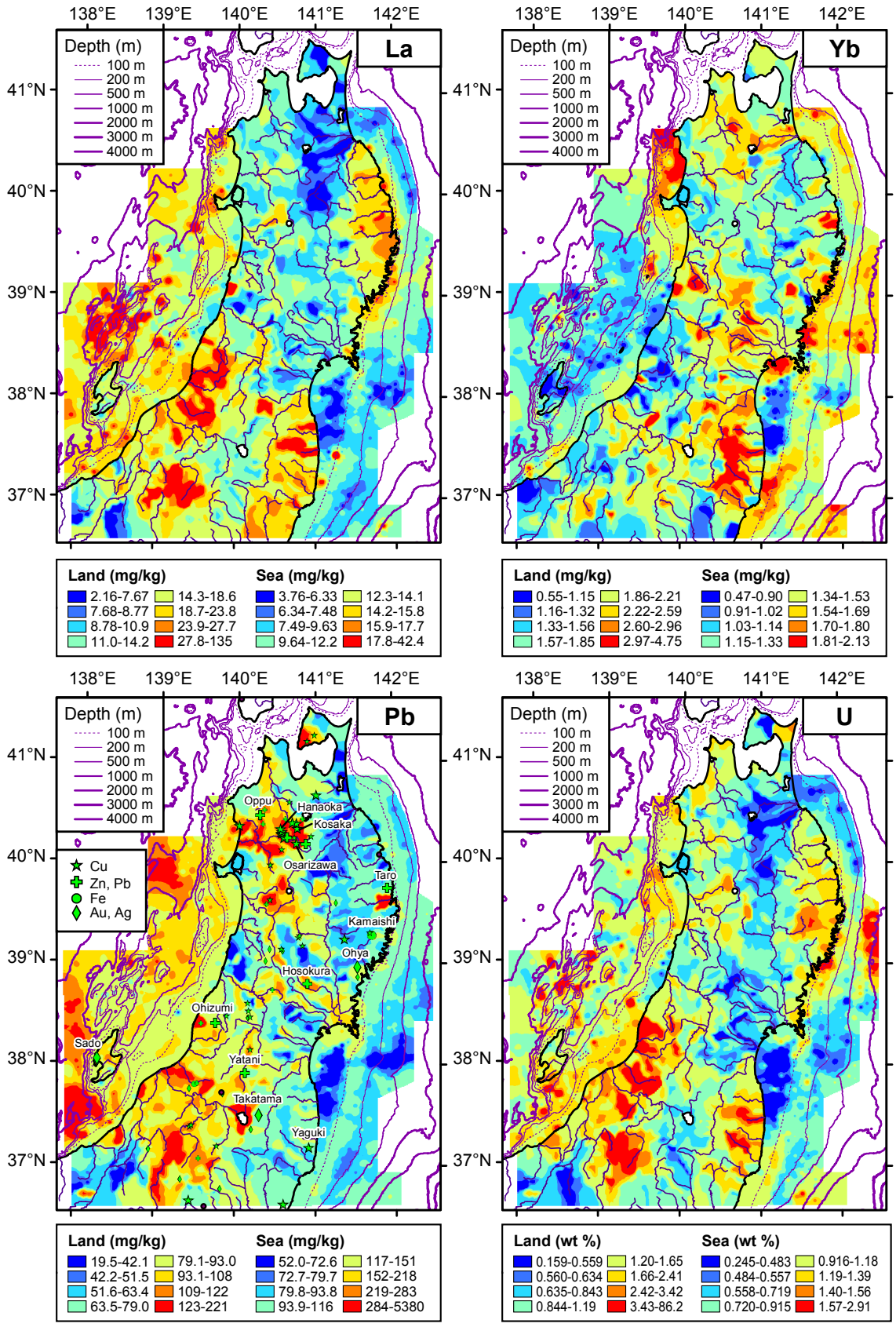

Fig. 4 Continued.

In contrast, the spatial distribution patterns of As, Cd, Sb, Hg, Pb, and Bi are strongly influenced not by geology but by mineral deposits. Certain Kuroko-type deposits, which are found at the Kosaka and Hanaoka mines within the Yoneshiro River watershed and the Taro mine in the Kitakami Mountains, greatly enhance Cu, Zn, Cd, Sb, Hg, Pb, and Bi concentrations in sediments. Skarn-type deposits, such as those of the Kamaishi and Yaoi mines, are associated with elevated Fe_2O_3 and Cu concentrations in sediments. The Au mine on Sado Island is the largest hydrothermal vein in Japan and shows elevated As concentrations in sediments. Therefore, geochemical maps in terrestrial areas are simply controlled by lithology and mineral deposits.

5. 2 Geochemical features of elemental concentrations in marine sediments

5. 2. 1 Spatial distributions of elements in marine environments

In the Pacific Ocean, MgO, Al_2O_3, CaO, Sc, TiO_2, V, MnO, Fe_2O_3, Co, Ga, and Sr are abundant in the sandy sediments on the shelf and slope off of Hachinohe. The area offshore from Kamaishi is relatively abundant in Li, Be, P_2O_5, K_2O, Cr, Ni, Rb, Y, Nb, Sb, Cs, Ba, REEs, Ta, Tl, Th, and U, although the areas of high enrichment in these elements are restricted to near the shore. Cu, Zn, As, Mo, Cd, Sn, Sb, Hg, Pb, and Bi are elevated in silt content on the shelf off of Ishinomaki. Coarse sediments on the shelf off of Shioyazaki and the southern part of Sendai Bay are depleted in all elements analyzed except for As and Ba. Silts collected from the continental slope have high concentrations of Li, V, Cr, Fe_2O_3, Ni, Cu, Zn, Nb, Mo, Cd, Sn, Sb, Cs, heavy REEs, Ta, Hg, Pb, Bi and U.

For the Sea of Japan, coarse sediments collected from the shelf and sea topographic highs are highly enriched in CaO and Sr. It is clear that these enrichments (especially in samples with CaO > 7.0 wt%) are caused by shell fragments and foraminiferal tests. Sandy sediments from the continental shelf are generally poor in almost all of the elements analyzed. However, sands on the shelf off of Noshiro are enriched in Al_2O_3, Sc, TiO_2, Fe_2O_3, Co, and heavy REEs; coarse sands on the shelf off of Mogami are abundant in As and Ba; coarse and fine sands on the edge of the shelf off of Niigata are enriched in As and Fe_2O_3; and coarse sands on the shelf off Joetsu are rich in Al_2O_3, P_2O_5, Sc, Fe_2O_3, Co, As, REEs, and Th. Silts and clays on the continental shelf off of Niigata are abundant in Li, P_2O_5, TiO_2, Cr, Ni, Cu, Nb, Cd, Sn, Cs, heavy REEs, Ta, Hg, Pb, Bi, and U. Sandy and silty sediments collected from the Sado Ridge have high concentrations of K_2O, Rb, and Cs, and especially of Be, Ba and light REEs. Clays from the Yamato Basin and the Toyama Trough are abundant in Li, MgO, P_2O_5, TiO_2, Cr, MnO, Co, Ni, Cu, As, Rb, Cs, Mo, Sn, Sb, Pb, Bi, and Tl. Thus, marine geochemical maps differ by area, and patterns are strongly associated with sediment grain sizes.

5. 2. 2 Variation of elemental concentrations in marine sediments with water depth

Figure 5 shows the mud contents and elemental concentrations of marine sediments from the Sea of Japan and the Pacific Ocean near Tohoku according to water depth. Except for the shallow water of Sendai Bay and the shelf offshore from the Niigata region, mud content in the Pacific Ocean increases gradually with water depth and steeply below 500 m, whereas mud content in the Sea of Japan increases steeply with water depth and becomes steady (90–100%) below depths of about 200–500 m. Correspondingly, changes in the elemental concentrations in sediments are similar to the systematic changes in mud content with water depth (see Cu and Cs in Fig. 5). The concentrations of many elements, such as MgO, Al_2O_3, K_2O, TiO_2, Fe_2O_3, vary greatly on the shelf (water depth (WD) = 0–200 m), but become constant below 200 m. Some elements present distinctive changes outside of this rule. Sediments collected around submarine topographic highs in the Sea of Japan (WD = 100–600 m) are abundant in Be, K_2O, Rb, Cs, Ba, and light REEs (La–Gd). The MnO, As and Mo concentrations increase steeply at depths below 500 m in the Sea of Japan (particularly the Toyama Trough and Yamato Basin). Cd, Hg and U concentrations are very high within 500–1,100 m in depth in both marine areas, but reach a constant low in deeper parts (>1,100 m) of the Sea of Japan.

6. Discussion

6. 1 Comparison of elemental abundances in stream and marine sediments between the Sea of Japan and the Pacific Ocean and with grain size

We have confirmed the geochemical features of terrestrial and marine environments of the Tohoku region using geochemical maps (Fig. 4). Figure 5 shows that the depositional or sedimentary environments systematically differ between the Sea of Japan and the Pacific Ocean. Next, we averaged the geochemical data to quantify the systematic differences in the chemical compositions of marine sediments. Figure 6 shows the median elemental concentrations of stream and marine sediments for both the Pacific Ocean and the Sea of Japan; these concentrations have been normalized to upper continental crust (UCC) values (Taylor and McLennan, 1995). The median is a robust estimation of the mean value that is less susceptible to outlier bias. Calculated median data are shown in Table 3. Stream sediments are rich in Sc, TiO_2, V, Cr, MnO, Fe_2O_3, Co, Zn, As and Sb but poor in Be, K_2O, Rb, Nb, Sn, Ta, Th, and U relative to UCC. As pointed out by Ujiie-Mikoshiba *et al*. (2006), stream sediments of the Tohoku region reflect the geochemical characteristics of igneous rocks in the orogenic arc. The UCC-normalized patterns of stream sediments on the Pacific Ocean side of Tohoku are similar to those on the Sea of Japan side. Sea of Japan sediments are somewhat abundant in K_2O, Rb, Mo, Cd, Cs, Ba, Tl, Pb, Bi, Th and U, which may be attributed to felsic

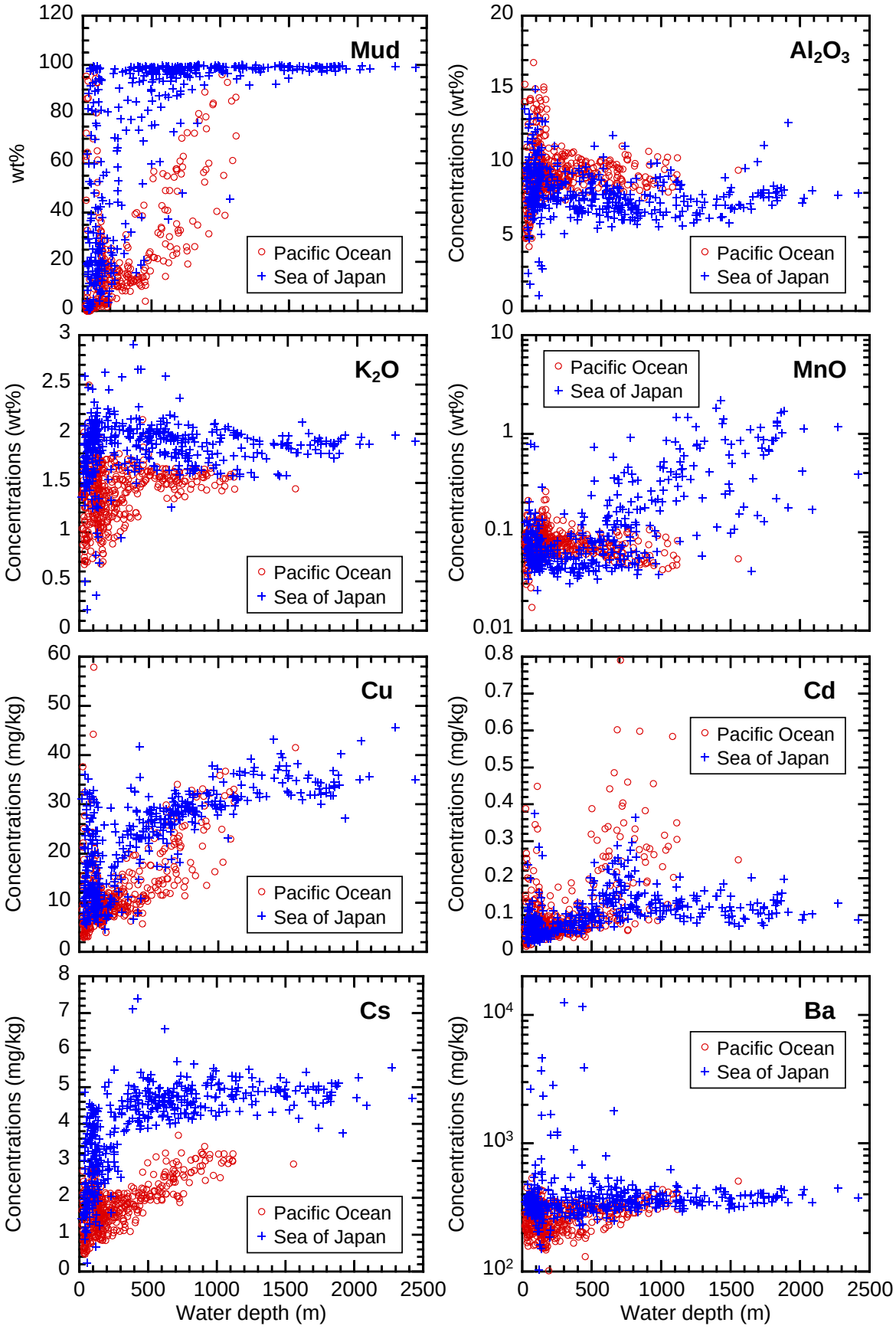

Fig. 5 Systematic change in mud contents and elemental concentrations in marine samples with changing water depth.

Table 3 Median elemental concentrations of marine and stream sediments.

Element	Pacific Ocean					Sea of Japan					
	Stream sed.	Marine sediment				Stream sed.	Marine sediment				
		All data	Coarse sed.	Fine sand	Silt		All data	Coarse sed.	Fine sand	Silt	Clay
	N=309	*N=439*	*N=115*	*N=249*	*N=75*	*N=346*	*N=418*	*N=36*	*N=92*	*N=79*	*N=211*
%											
Na_2O	2.21	2.95	2.67	2.96	3.50	2.17	3.65	2.54	2.84	3.30	4.38
MgO	3.00	2.78	2.80	2.74	2.86	2.50	4.07	2.97	3.62	3.87	4.24
Al_2O_3	11.5	9.23	9.32	9.31	9.04	10.4	7.84	7.18	8.83	8.31	7.60
P_2O_5	0.11	0.098	0.090	0.097	0.12	0.12	0.14	0.11	0.12	0.14	0.16
K_2O	1.32	1.44	1.19	1.48	1.56	1.67	1.90	1.64	1.92	1.93	1.90
CaO	3.12	3.57	3.83	3.66	2.80	2.24	1.06	3.12	2.33	1.16	0.88
TiO_2	0.77	0.46	0.43	0.46	0.46	0.67	0.47	0.31	0.46	0.52	0.46
MnO	0.14	0.076	0.085	0.077	0.059	0.12	0.072	0.071	0.066	0.057	0.12
Fe_2O_3	6.80	5.01	5.31	4.97	4.92	5.63	4.44	3.96	5.84	5.00	4.17
mg/kg											
Li	20	19	16	19	28	22	38	24	30	38	40
Be	1.1	0.97	0.80	1.0	1.1	1.2	1.4	1.0	1.4	1.4	1.3
Sc	19	13	14	13	12	12	8.5	6.1	9.9	9.7	8.0
V	137	81	74	81	90	108	99	56	83	96	102
Cr	47	38	32	39	50	45	55	30	46	54	58
Co	16	8.3	9.1	8.2	7.5	12	10	6.0	10	11	9.0
Ni	16	14	11	14	21	16	28	14	16	23	31
Cu	26	10	7.1	10	23	23	26	9.0	12	22	30
Zn	110	75	68	72	94	124	99	64	87	107	102
Ga	16	12	12	13	13	16	14	11	13	15	14
As	10	4.9	5.6	4.6	5.6	8.9	14	21	14	15	13
Rb	41	36	29	37	44	55	57	52	56	56	58
Sr	164	198	196	205	162	146	123	209	172	123	109
Y	19	15	13	15	16	17	12	11	15	13	12
Nb	6.1	4.2	3.1	4.3	5.5	6.2	5.7	3.4	5.1	6.1	5.8
Mo	1.3	0.81	0.76	0.72	1.3	1.5	1.3	0.76	0.89	1.1	1.9
Cd	0.13	0.072	0.065	0.066	0.22	0.20	0.093	0.041	0.054	0.079	0.12
Sn	1.7	1.0	0.80	1.0	1.4	1.9	2.1	1.2	1.4	2.2	2.3
Sb	0.59	0.42	0.37	0.43	0.71	0.60	0.70	0.45	0.50	0.53	0.96
Cs	2.2	1.8	1.2	1.8	2.6	2.8	4.3	1.9	2.8	3.8	4.8
Ba	348	260	211	276	287	423	344	317	343	328	352
La	13	9.8	7.7	10	12	14	14	12	15	14	14
Ce	26	19	16	19	21	26	23	23	31	26	20
Pr	3.4	2.5	2.0	2.6	2.9	3.5	3.3	2.7	3.7	3.5	3.2
Nd	14	11	8.6	11	12	14	13	11	15	14	13
Sm	3.3	2.4	2.1	2.5	2.7	3.1	2.8	2.3	3.2	3.1	2.7
Eu	0.88	0.72	0.70	0.74	0.68	0.82	0.64	0.59	0.81	0.68	0.60
Gd	3.3	2.4	2.1	2.4	2.6	3.0	2.6	2.1	3.0	2.8	2.6
Tb	0.60	0.44	0.39	0.44	0.49	0.55	0.45	0.36	0.51	0.49	0.43
Dy	3.2	2.4	2.1	2.4	2.6	2.9	2.2	1.8	2.6	2.5	2.2
Ho	0.64	0.48	0.42	0.48	0.52	0.57	0.42	0.34	0.50	0.47	0.40
Er	1.9	1.4	1.3	1.4	1.6	1.7	1.2	1.0	1.5	1.4	1.2
Tm	0.31	0.23	0.20	0.23	0.26	0.28	0.19	0.16	0.23	0.22	0.19
Yb	1.9	1.4	1.3	1.5	1.6	1.7	1.2	0.95	1.4	1.4	1.2
Lu	0.29	0.22	0.19	0.22	0.25	0.26	0.18	0.14	0.20	0.20	0.17
Ta	0.49	0.33	0.24	0.33	0.44	0.49	0.50	0.31	0.41	0.54	0.52
Hg	0.030	0.047	0.027	0.047	0.11	0.030	0.040	0.030	0.045	0.080	0.040
Tl	0.35	0.28	0.21	0.29	0.32	0.51	0.45	0.34	0.37	0.45	0.47
Pb	17	15	13	14	18	26	39	24	28	35	45
Bi	0.19	0.14	0.090	0.14	0.26	0.24	0.62	0.27	0.30	0.55	0.73
Th	3.7	2.8	1.9	2.9	3.6	4.6	4.3	3.8	4.6	5.0	4.1
U	1.1	0.78	0.61	0.78	1.2	1.3	1.1	0.87	1.2	1.2	0.97

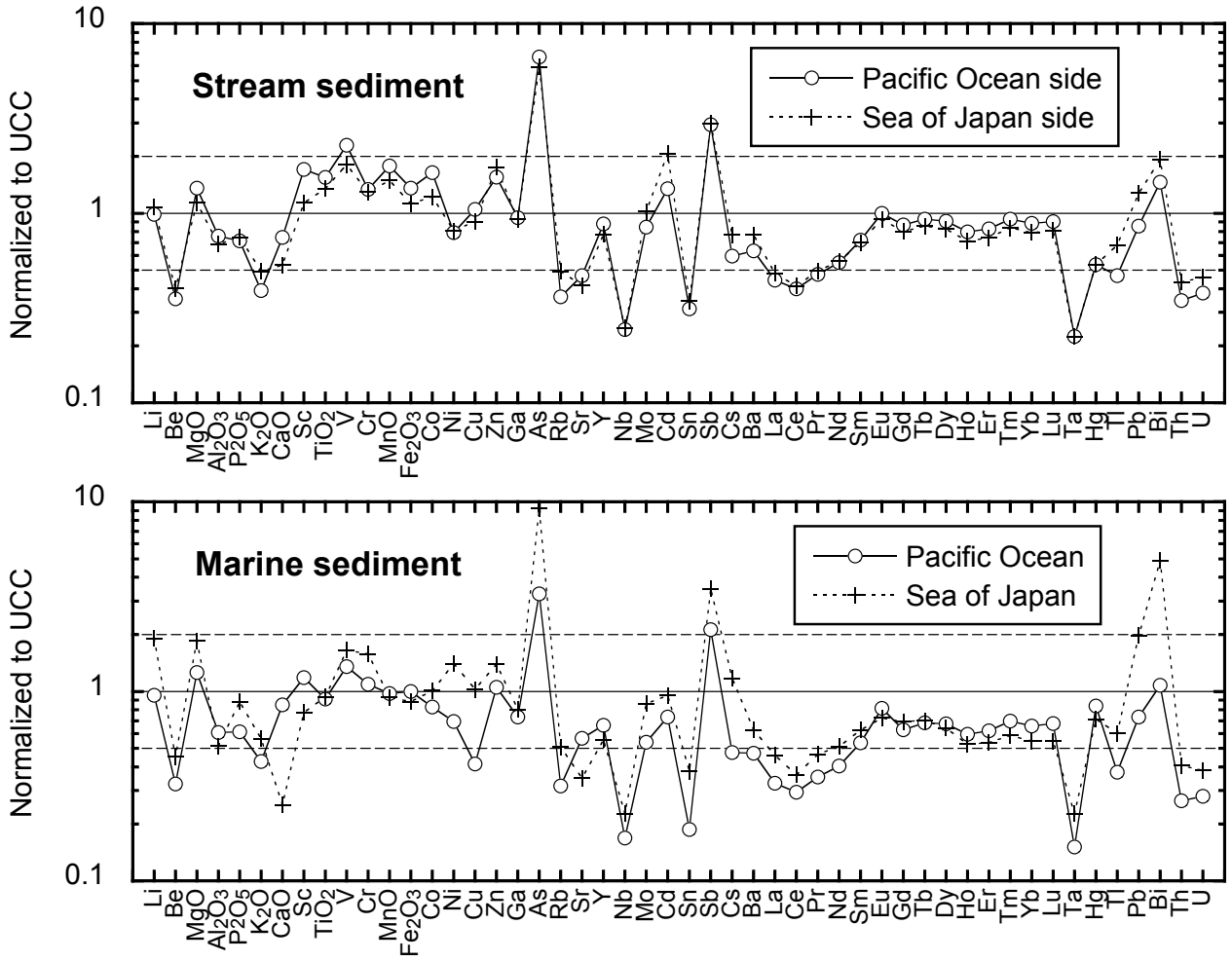

Fig. 6 Chemical compositions of stream sediments and marine sediments normalized to the upper continental crust.

igneous rocks and metalliferous deposits associated with Neogene felsic volcanic rocks. UCC-normalized values for marine sediments are systematically lower than those of stream sediments, although they have fundamentally similar geochemical features. Marine sediments of the Sea of Japan are relatively abundant in Li, MgO, P_2O_5, K_2O, Cr, Ni, Cu, Zn, As, Rb, Mo, Sn, Cs, Ba, light REEs, Tl, Pb, Bi, Th and U, but scarce in CaO, Sc, and Sr compared to those of the Pacific Ocean.

Figure 7 shows the median elemental concentrations of marine sediments according to grain size and region, normalized to those of stream sediments. The classification of grain size is the same as that used in Fig. 3. Median data for grain sizes and regions are also summarized in Table 3. In the Pacific Ocean, MgO, Al_2O_3, CaO, Sc, TiO_2, V, Fe_2O_3, Ga, and Eu concentrations are similar, whereas the concentrations of other elements, especially Li, Cu, Cd, Cs, Hg, and Bi, increase with decreasing grain size. In the Sea of Japan, many elemental concentrations increase with decreasing grain size. There are no systematic changes in K_2O, Rb, and Ba concentrations. Al_2O_3, Fe_2O_3, Ga, REEs, Th, and U concentrations are high in fine sand and silt but low in coarse sediment and clay. Arsenic is highly abundant in coarse sediment, and MnO is highly enriched in clay. CaO and Sr concentrations decrease systematically with decreasing grain size. In summary, geochemical differences in marine sediments between the Pacific Ocean and the Sea of Japan are larger than those in stream sediments. Furthermore, chemical compositions of marine sediments change systematically with grain size.

6. 2 Two-way ANOVA applied to quantitatively assess factors controlling elemental concentrations in marine sediments

The regional geochemical differences identified in marine sediments are inferred to be caused by factors such as differing amounts of terrestrial sediment discharge to the coast, denudation of local marine basement rocks, and the occurrence of relict sediments. Geochemical variations in sediment with grain size may indicate the effects of dilution with quartz and calcareous materials, the enhancement of heavy elements through early

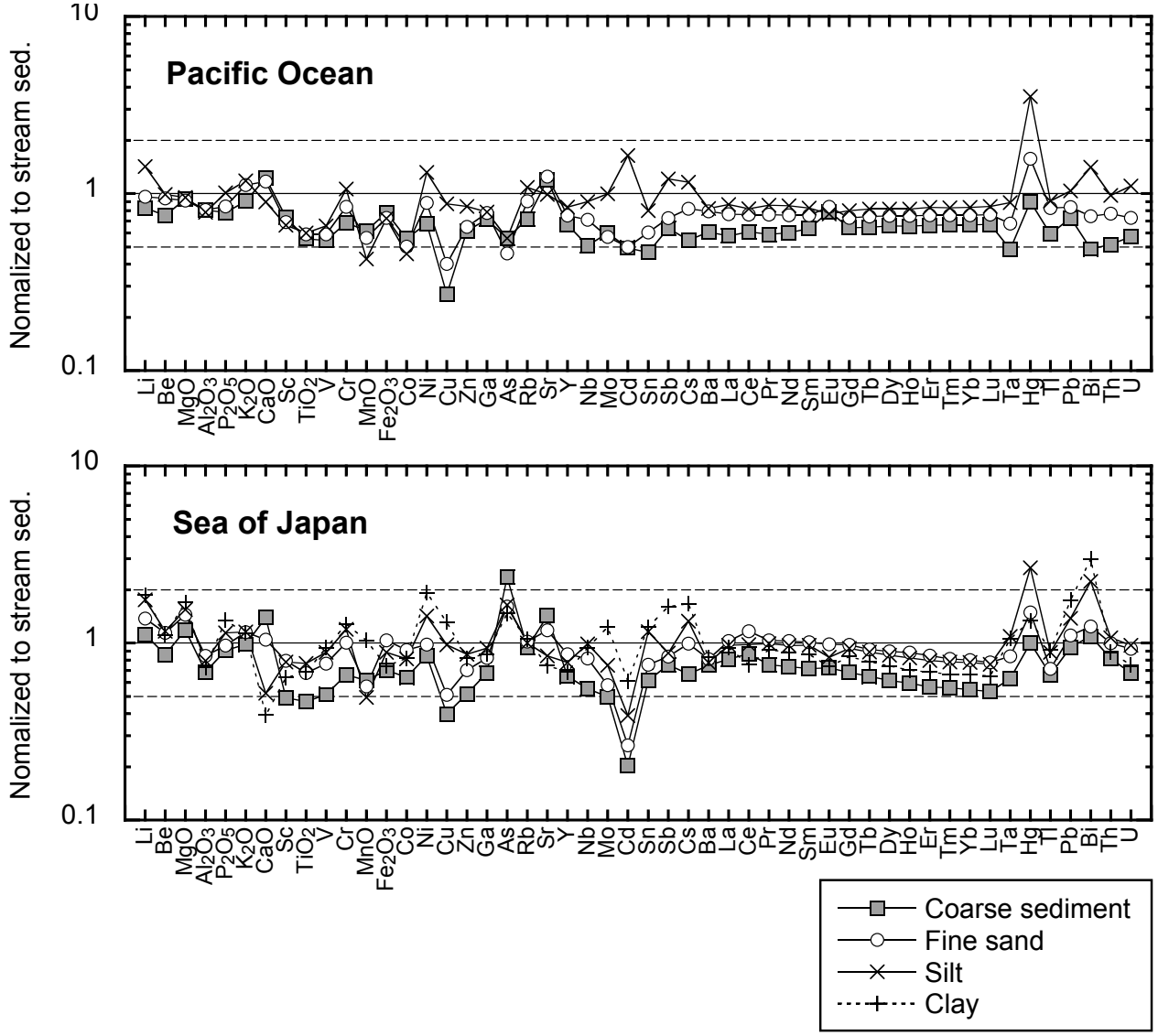

Fig. 7 Chemical variations of coarse sediments, fine sands, silts and clays in marine sediments normalized to the adjacent terrestrial sediments.

diagenetic process, increasing clay contents. Next, we have investigated which controlling factor is dominant for each element using two-way analysis of variance (ANOVA).

For this process, we closely followed the methods described by Ohta *et al*. (2007). The Ekuseru-Toukei 7.0 software (ESUMI Corp. Ltd.) was used for statistical analysis. We generally assumed that geochemical data followed either normal distribution or log-normal distribution. However, geochemical data do not strictly follow either of these distribution patterns in most cases (Ohta *et al*., 2007). Therefore, as a second approach, data with a symmetrical distribution were used for ANOVA, i.e., data sets with data skewness close to zero were used. Table 4 shows the skewness of our geochemical data and the format of these data used for ANOVA. Samples were classified into seven sub-groups, as shown in Table 3: coarse sediments, fine sand, and silt in the Pacific Ocean; and coarse sediments, fine sand, silt, and clay in the Sea of Japan. Unfortunately, clay was not found in appreciable amounts in the Pacific Ocean; therefore, ANOVA provides only semi-quantitative results. Nonetheless, the findings obtained through ANOVA are informative.

Table 5 shows the variance ratios (F), probabilities (p), and the size effects (η^2) of regional differences (factor A), grain size (factor B), and the interaction effects (factor A × factor B), which were estimated through two-way ANOVA. When the p value is lower than 0.01, we conclude that the effect of that factor is significant. However, Table 4 demonstrates that in most cases, each factor is statistically significant ($p < 0.01$). This finding can be attributed to very small difference detected to be

Table 4 Skewness of unchanged and log-transformed data.

Element	Skewness		Data transformation for ANOVA
	Raw	Log	
MgO	−0.26	−1.52	Unchanged
Al_2O_3	0.52	−1.71	Unchanged
P_2O_5	1.79	0.24	Log-transformed
K_2O	−0.35	−1.62	Unchanged
CaO	5.85	0.29	Log-transformed
TiO_2	1.18	−1.95	Unchanged
MnO	4.57	1.91	Log-transformed
Fe_2O_3	2.04	−0.15	Log-transformed
Li	0.21	−0.34	Unchanged
Be	1.93	−0.46	Log-transformed
Sc	1.31	−0.43	Log-transformed
V	−0.09	−2.11	Unchanged
Cr	1.80	−0.82	Log-transformed
Co	1.64	−1.52	Log-transformed
Ni	2.62	0.07	Log-transformed
Cu	0.55	−0.18	Log-transformed
Zn	−0.84	−1.23	Unchanged
Ga	−1.37	−3.82	Unchanged
As	4.21	0.42	Log-transformed
Rb	0.40	−0.81	Unchanged
Sr	7.37	1.41	Log-transformed
Y	0.14	−0.49	Unchanged
Nb	−0.4	−1.61	Unchanged
Mo	6.77	1.35	Log-transformed
Cd	2.92	0.50	Log-transformed
Sn	0.47	−0.31	Log-transformed
Sb	1.21	0.07	Log-transformed
Cs	0.38	−0.41	Unchanged
Ba	15.47	2.93	Log-transformed
La	2.21	−0.18	Log-transformed
Ce	3.47	0.57	Log-transformed
Pr	2.36	−0.18	Log-transformed
Nd	2.44	−0.17	Log-transformed
Sm	2.13	−0.29	Log-transformed
Eu	2.01	0.54	Log-transformed
Gd	1.55	−0.47	Log-transformed
Tb	0.90	−0.59	Log-transformed
Dy	0.38	−0.65	Unchanged
Ho	0.17	−0.57	Unchanged
Er	0.09	−0.57	Unchanged
Tm	0.09	−0.53	Unchanged
Yb	0.08	−0.53	Unchanged
Lu	0.05	−0.56	Unchanged
Ta	−0.29	−3.4	Unchanged
Hg	5.42	−0.16	Log-transformed
Tl	−0.09	−0.93	Unchanged
Pb	0.64	−0.03	Log-transformed
Bi	0.96	−0.41	Log-transformed
Th	1.16	−0.75	Log-transformed
U	0.97	−0.3	Log-transformed

significant in the case of a large sample size ($N = 857$). In such cases, η^2 can be used for a plausible estimate of the p value irrespective of the number of samples (Richardson, 2011; Fritz *et al*., 2012). In this study, we conclude that 1) a factor with $\eta^2 \geq 0.06$ has a significant influence on changes in chemical compositions, and 2) a factor with a higher η^2 score indicates a more significant effect on chemical compositions (Fritz *et al*., 2012).

The "interaction effect" refers to the effect of one factor on another factor, i.e., the two factors affect the data synergistically. The η^2 score of the interaction effect is lower than 0.06 for the entire data set (Table 5). It is therefore concluded that these factors affect the chemical compositions of sediments independently. ANOVA also suggests that 1) the grain size effect is significant for almost all elements except for Al_2O_3, TiO_2, Sc, Co, As, Rb, and Ba in marine sediments, and 2) grain size has stronger influence on the concentrations of 33 elements than do regional differences. The regional difference effect is significant for 25 elements, but only 14 elements, such as MgO and K_2O, are more dominantly affected by regional differences than by grain size. Consequently, the ANOVA results caution that grain size obscures geochemical information of sediment origin in most cases. Therefore, we have divided the study area into regions in which marine sediments are roughly similar in terms of grain size to elucidate the processes of particle transport from land to sea and the influence of local marine geology.

6.3 Geochemical features of marine sediments in the Pacific Ocean

6.3.1 Influence of local marine geology on marine geochemical maps

Coarse sands distributed on the continental shelf off of Hachinohe are highly abundant in elements that are enriched in mafic volcanic rocks such as Al_2O_3, CaO, MnO, and Fe_2O_3, and scarce in elements enriched in felsic igneous rocks such as K_2O, Rb, Cs, Ba, REEs, and Th. In contrast, in the Sea of Japan, coarse sediments are relatively depleted in many elements, except for CaO, Sr and As (Fig. 7). Small rivers flow to the coastline of the Hachinohe area. Furthermore, most coarse sediments were collected from depths below wave base. Water movement, such as fair-weather and storm waves and coastal current, is able to move sandy sediments at water depths of less than 50–80 m (Saito, 1989). Therefore, the transport processes of modern sediments from land to sea are not the cause of the enrichment of the above-mentioned elements. Arita and Kinoshita (1978) and Nishimura and Saito (2016) reported that the sandy sediments of the Pacific Ocean contain large amounts of volcanic rock fragments and heavy minerals such as augite, hypersthene and hornblende. In fact, the marine geological map shows that Miocene volcanic rocks are exposed in the region offshore from Hachinohe (Fig. 2). Therefore, we assume that these coarse sands were produced by the denudation of Miocene volcanic rocks on the continental shelf off of

Table 5 Variance ratios (F), probabilities (p), and size effects (η^2) of two-way ANOVA applied to the unchanged and log-transformed data.

Element	F			p			η^2			Dominant factor
	A	B	A×B	A	B	A×B	A	B	A×B	
MgO	302	44	5	<0.01	<0.01	<0.01	**0.154**	**0.068**	0.008	Regional
Al_2O_3	48	11	11	<0.01	<0.01	<0.01	0.045	0.030	0.032	none
P_2O_5	105	84	2	<0.01	<0.01	0.15	**0.061**	**0.146**	0.003	Grain size
K_2O	372	48	2	<0.01	<0.01	0.13	**0.217**	**0.084**	0.003	Regional
CaO	75	189	19	<0.01	<0.01	<0.01	0.032	**0.243**	0.025	Grain size
TiO_2	<1	14	13	0.44	<0.01	<0.01	0.001	0.046	0.041	none
MnO	<1	52	0.7	0.74	<0.01	0.56	0.000	**0.147**	0.002	Grain size
Fe_2O_3	5	32	15	0.03	<0.01	<0.01	0.005	**0.096**	0.045	Grain size
Li	418	270	3	<0.01	<0.01	0.05	**0.111**	**0.216**	0.002	Grain size
Be	383	81	9	<0.01	<0.01	<0.01	**0.207**	**0.131**	0.014	Regional
Sc	200	23	19	<0.01	<0.01	<0.01	**0.142**	0.049	0.041	Regional
V	1	44	3	0.34	<0.01	0.05	0.001	**0.123**	0.007	Grain size
Cr	22	113	1	<0.01	<0.01	0.22	0.020	**0.231**	0.004	Grain size
Co	105	3	8	<0.01	0.03	<0.01	**0.098**	0.009	0.022	Regional
Ni	56	214	2	<0.01	<0.01	0.13	0.025	**0.284**	0.003	Grain size
Cu	15	443	4	<0.01	<0.01	0.01	0.005	**0.436**	0.004	Grain size
Zn	40	103	13	<0.01	<0.01	<0.01	0.028	**0.216**	0.028	Grain size
Ga	14	88	25	<0.01	<0.01	<0.01	0.010	**0.198**	0.057	Grain size
As	694	16	4	<0.01	<0.01	<0.01	**0.363**	0.025	0.007	Regional
Rb	299	19	5	<0.01	<0.01	<0.01	**0.194**	0.036	0.009	Regional
Sr	2	104	15	0.21	<0.01	<0.01	0.001	**0.218**	0.031	Grain size
Y	15	80	10	<0.01	<0.01	<0.01	0.012	**0.200**	0.024	Grain size
Nb	34	177	1	<0.01	<0.01	0.22	0.020	**0.315**	0.003	Grain size
Mo	8	81	<1	<0.01	<0.01	0.44	0.006	**0.181**	0.002	Grain size
Cd	128	189	27	<0.01	<0.01	<0.01	**0.085**	**0.378**	0.055	Grain size
Sn	249	331	<1	<0.01	<0.01	0.77	**0.086**	**0.277**	0.001	Grain size
Sb	0.03	109	11	0.87	<0.01	<0.01	0.000	**0.233**	0.023	Grain size
Cs	428	328	3	<0.01	<0.01	0.02	**0.100**	**0.230**	0.002	Grain size
Ba	129	18	3	<0.01	<0.01	0.04	**0.116**	0.048	0.007	Regional
La	342	66	7	<0.01	<0.01	<0.01	**0.210**	**0.122**	0.013	Regional
Ce	329	90	10	<0.01	<0.01	<0.01	**0.238**	**0.195**	0.022	Regional
Pr	339	82	7	<0.01	<0.01	<0.01	**0.208**	**0.151**	0.013	Regional
Nd	299	87	7	<0.01	<0.01	<0.01	**0.192**	**0.168**	0.014	Regional
Sm	207	96	7	<0.01	<0.01	<0.01	**0.144**	**0.201**	0.015	Grain size
Eu	11	91	17	<0.01	<0.01	<0.01	0.009	**0.225**	0.042	Grain size
Gd	126	92	7	<0.01	<0.01	<0.01	**0.097**	**0.213**	0.017	Grain size
Tb	45	96	8	<0.01	<0.01	<0.01	0.037	**0.238**	0.021	Grain size
Dy	12	87	10	<0.01	<0.01	<0.01	0.010	**0.230**	0.026	Grain size
Ho	<1	87	8	0.4	<0.01	<0.01	0.001	**0.225**	0.022	Grain size
Er	14	89	8	<0.01	<0.01	<0.01	0.011	**0.220**	0.020	Grain size
Tm	34	90	7	<0.01	<0.01	<0.01	0.027	**0.214**	0.017	Grain size
Yb	52	86	7	<0.01	<0.01	<0.01	0.041	**0.202**	0.016	Grain size
Lu	87	85	6	<0.01	<0.01	<0.01	**0.065**	**0.191**	0.014	Grain size
Ta	78	139	1.3	<0.01	<0.01	0.26	0.045	**0.240**	0.002	Grain size
Hg	<1	71	2.2	0.85	<0.01	0.09	0.000	**0.198**	0.006	Grain size
Tl	183	58	4	<0.01	<0.01	0.01	**0.106**	**0.100**	0.006	Regional
Pb	937	165	2	<0.01	<0.01	0.21	**0.214**	**0.113**	0.001	Regional
Bi	448	163	2	<0.01	<0.01	0.11	**0.142**	**0.156**	0.002	Grain size
Th	314	88	5	<0.01	<0.01	<0.01	**0.184**	**0.155**	0.009	Regional
U	133	84	14	<0.01	<0.01	<0.01	**0.099**	**0.187**	0.031	Grain size

The A, B and A×B indicate the regional effect, the grain size effect, and the interaction effect, respectively. Bold phase type means that η^2 is larger than 0.06.

Hachinohe during regression and transgression.

6. 3. 2 Particle transport from land to sea and within the marine environment in the Pacific Ocean

The distribution of silts in Sendai Bay is evidence for the input of modern sediments from rivers because major rivers that drain into the Pacific Ocean flow into Sendai Bay (Table 1). The concentrations of many elements, such as Cu, As, Cd, Yb, and Pb, in silt from Sendai Bay are higher than those in near-shore sandy sediments because of the grain size effect. Silts on the deep continental slope of the Pacific Ocean also have high concentrations of Li, Cr, Ni, Cu, Nb, Mo, Cd, Sn, Sb, Cs, Ta, Hg, Bi, and U, which can be explained by the same effect. The concentrations of many elements in silt both in Sendai Bay and on the continental slope are similar. However, the Zn, As, Hg, and Pb concentrations of silts in Sendai Bay are half as high as those of silts on the continental slope. Their enrichment may be attributed to anthropogenic activity or the supply of ore minerals from the Hosokura Mine.

The coarse sediments distributing on the continental shelf off of Shioyazaki are remarkably depleted in most elements except for As and Ba. Dilution effects caused by preferential enrichment in quartz and feldspar, which may be supplied from granitic rocks of the nearby Abukuma Mountains, may be the cause. The same phenomenon is observed on the continental shelf off of the Atsumi Peninsula of the Tokai Region (Ohta *et al*., 2007). Quartz and feldspar generally do not become small grains because of their resistance to physical weathering processes (e.g., Goldich, 1938). Consequently, these minerals are not transported by water movement to the degree that small grains of minerals such as mica, biotite, and amphibole are, and selectively accumulate on the continental shelf. This important mineralogical fractionation obscures sediment origin information.

The spatial distributions of many elements, such as K_2O, Rb, Nb, REEs, and Th, are continuous between the Kitakami Mountains and the nearby the coast off of Kamaishi (e.g., K_2O, La, and U in Fig. 4). As explained above, marine sediments in the Pacific Ocean in this region are influenced by mafic volcanic rocks (Nishimura and Saito, 2016), which are associated with lower Li, K_2O, Rb, Cs, Ba, Nb, REEs, Ta, and Th concentrations in sediments. Therefore, the influence of sediments that originated from granitic intrusions and accretionary complexes becomes apparent. However, the rivers that flow through the Kitakami Mountains to the coast near Kamaishi are small, and their sediment yields are low. In addition, most of the marine sediments sampled were collected from water depths of 50–150 m, below wave base. Accordingly, these samples are interpreted as relict sediments that originated from coastal erosion and/or denudation of granitic rocks and accretionary complexes during regression and transgression.

The wide distribution of fine sands on the continental shelf and slope off of Kamaishi is clearly explained by the deposition of relict sediments because most of these samples were deposited below the depth of wave base and away from the shore (Fig. 3). Noda and TuZino (2007) reported that sandy sediments on the edge of the continental shelf and on the continental slope are transported gradually by a gravity to a deeper area offshore from Nemuro, Hokkaido, Japan, which results in the formation of numerous gullies on the slope. However, there are few submarine canyons in the Pacific Ocean near the Tohoku region except for in the region off of Kamaishi (Yashima *et al*., 1982; Shimamura, 2008). Therefore, sediments may be conveyed to deeper areas via massive submarine landslides or sheet flows. Otherwise, these sediments may be produced by denudation of basement rocks such as Neogene sedimentary rocks (Fig. 2). Figure 8 shows that the median concentrations of elements in fine sands are classified with water depths, which are normalized to stream sediments on the Pacific Ocean side. We followed the convention of dividing the samples into four groups: the shelf (WD = 0–100 m), the edge of the shelf (WD = 100–200 m), the upper slope (WD = 200–500 m), and the lower slope (WD = 500–1,000 m). The shelf was an erosional region during regression and subsequently shifted to a depositional environment during transgression. The edge of the shelf was under depositional conditions even during transgression. The upper slope has thin Quaternary sediments overlying Miocene sediments (Okamura and Tanahashi, 1983). The lower slope is a deep-sea terrace. Figure 8 shows that normalized patterns of fine sediments in the Pacific Ocean are fairly consistent; their mean chemical compositions are similar to those of terrestrial areas influenced by orogenic belt volcanism, as explained above. Furthermore, no significant differences are apparent among samples; marine sediments in the Pacific Ocean have very homogenous geochemical features. Enrichment in Cr, Fe_2O_3, Cu, Cd, Sb, Cs, and Hg in sandy sediments collected from sea-floor depth of over 500 m (Fig. 3) is explained by the increase in the proportion of silts. These results suggest that fine sands were deposited on the continental shelf under the influence of volcanic activity during a regression/transgression and have been transported from the continental shelf to the deep sea by gravity currents. From geochemical mapping of the Pacific Ocean, we observe two kinds of particle transport, i.e., present and past particle transportation, from land to sea.

6. 4 Geochemical features of marine sediments in the Sea of Japan

6. 4. 1 Particle transport processes from land to marine environments in the Sea of Japan

Sediments on the continental shelf off of Noshiro are expected to be influenced by Kuroko deposits because there are many geochemical anomalies found in the watershed area of the Yoneshiro River (Cu, Cd, and Pb in Fig. 4). Fine sands in the region off of Noshiro are abundant in Al_2O_3, Sc, TiO_2, Fe_2O_3, Co, and heavy REEs,

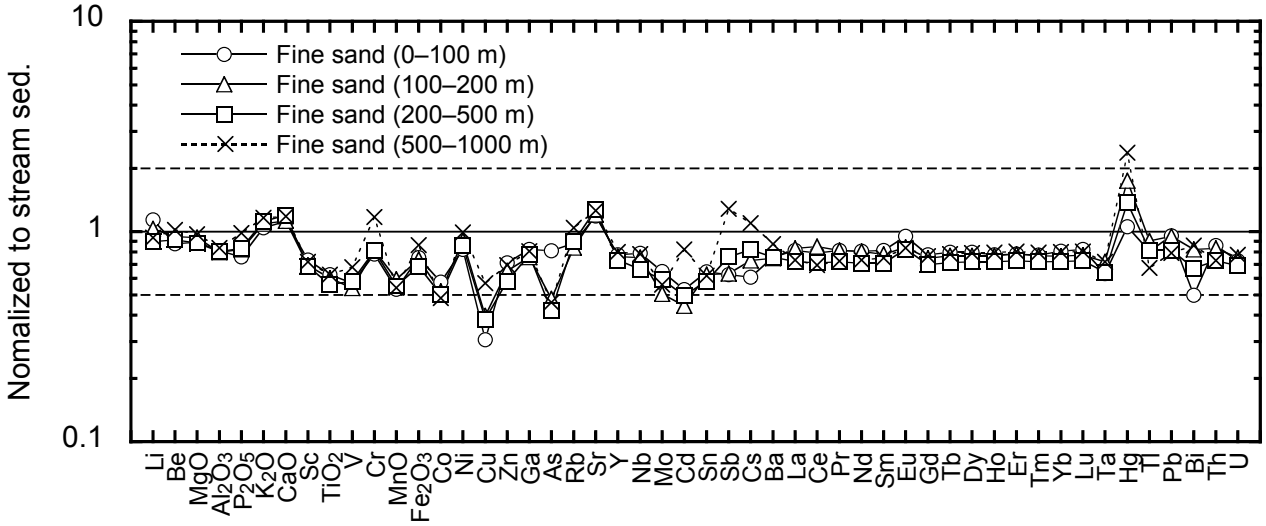

Fig. 8 Chemical variations of fine sands in the Pacific Ocean normalized to the adjacent terrestrial sediments.

but scarce in Cu, Zn, As, Cd, Sb, Pb, and Bi. Ohta *et al*. (2010) have discussed the transport processes of mining ores from the Kuroko deposits in the Yoneshiro River watershed to the coast. They concluded that sulfide ores have been oxidized and are releasing heavy metals during weathering and transportation. Based on those results, fine sands in the region offshore from Noshiro are inferred to have originated from mafic volcanic rocks in the northern Tohoku region and scarcely contain mining ores.

Silts and clays on the continental shelf off of Niigata are modern sediments supplied primarily by the Shinano and Agano Rivers because the sediment discharge yields of these rivers are the highest in the study area (Table 1). The spatial distributions of Be, K_2O, Rb, Sn, light REEs, Th, and U are continuous between the watershed of the Ara River and the coast because granitic rocks and accretionary complexes underlie the watershed area. However, these elements are less abundant in the estuarine regions of the Shinano and Agano Rivers because volcanic rocks are the dominant lithology of these river systems. Characteristically, Li, MgO, P_2O_5, V, Cr, Ni, Ga, Nb, Mo, Cs, Pb and Bi are more abundant in clay samples from far offshore and notably less abundant in silt from near the shore. These distribution patterns can be simply explained by the grain size effect. Several samples from the estuarine region of the Agano River are highly enriched in Cu, Zn, As, Cd, and Hg. This enrichments may be influenced by metalliferous deposits distributed in the watershed of the Agano River. As in the examples noted above, it must be considered that the spatial distributions of elemental concentrations are not always continuous between land and sea. Nevertheless, the influence of material input from land to sea is evident.

6. 4. 2 Relict sediments on the continental shelf

Coarse and fine sands are distributed on the continental shelf off of Mogami and Joetsu and on the edge of the continental shelf off of Niigata. These sandy sediments are poor in many elements, with the exceptions of Fe_2O_3 and As. Ikehara *et al*. (1994a, b) and Katayama *et al*. (1994) reported that sand particles in these regions contain quartz coated in Fe hydroxides, which are interpreted as relict sediments because fresh modern sand is not coated. The Fe hydroxide-coated quartz grains absorb As efficiently over long periods (e.g., Sullivan and Aller, 1996). Enrichment of As in sandy sediments collected from the southern part of Sendai Bay is also explained by this mechanism, because Nishimura and Saito (2016) found quartz coated with Fe hydroxides (stained quartz) in the sandy sediments of this region. Arsenic is supplied to coastal seas mainly in the dissolved phase through rivers and is precipitated in coastal sediments (Ohta *et al*., 2015). There are more As-enriched sandy sediments in the Sea of Japan because many major rivers flow into this sea (Table 1).

6. 4. 3 Hemipelagic conditions in deep sea basins

Half of sediments in the Sea of Japan consist of clay, which is mainly deposited in deep-sea basins such as the Yamato Basin and Toyama Trough. These clays are rich in elements such as MnO, Cr, Ni, Cu, As, Mo, Sb, and Pb. Terashima *et al*. (1995b) and Imai *et al*. (1997) have pointed out that enrichments of these elements are caused by early diagenetic processes. These elements were released into pore water at greater depths in sediments under reducing conditions, diffused upward, and finally precipitated with Mn oxide under oxic condition (e.g., Shaw *et al*., 1990). These deep-sea basins would be oxidative enough to cause Mn oxide precipitation because MnO concentrations are very high in sediments, and an oxygen-rich water mass (the Japan Sea Proper Water) covers the deep parts of the Sea of Japan (Gamo *et al*., 1986).

6. 4. 4 Influence of local marine geology on marine geochemical maps: particularly extreme enrichment of Ba caused by barite deposition

Figures 5 and 6 show that marine sediments in the Sea of Japan are rather enriched in Li, Be, K_2O, Rb, Nb, Cs, Ba, light REEs, Ta, Th, and U compared to those in the Pacific Ocean in this region and sediments of the adjacent terrestrial areas. These elemental concentrations are particularly high in sediments around the Sado Ridge, Awashima Island, the Torimi-Guri Bank, and the Shin-Guri Bank (Ba and La in Fig. 4). The characteristics of these sediments would be controlled by local marine geology because these places are distant from terrestrial areas and the sediments are of various grain sizes. To highlight the signatures of these sediments, in Fig. 9, we illustrate the distributions of outliers in Be, Ba and La associated with marine geological maps at 1:200,000 scale (Okamura *et al*., 1994, 1995a, 1996a, b). The threshold value for each element was determined by employing the Smirnov–Grubbs test for the original data at the 95% confidence level to identify outliers (Grubbs, 1969). Most of these outliers plot near marine faults associated with basement rocks. The upper surfaces of submarine topographic highs consist mainly of Middle Miocene–Pliocene siltstone called the Hirase Group (Okamura *et al*., 1995a, b). These strata have been uplifted from the seafloor by reverse faults that underwent inversion during the Late Pliocene to Quaternary (Okamura, 2010). Nakajima et al. (1995) suggest that sediments around these topographic highs formed through denudation of basement rocks. The Hirase Group corresponds to Miocene–Pliocene siltstone with dacitic tuff distributed in the adjacent terrestrial area. Therefore, these marine sediments would mainly reflect the geochemistry of the Hirase Group.

However, the spatial distribution of the outliers in Ba concentration do not correspond to those of Be and La concentrations. In particular, extremely high Ba concentrations of 2,000–15,000 mg/kg cannot be explained by regional geology. Barite nodules are known from the submarine topographic highs of the Sado Ridge and the Shin-Guri, Torimi-Guri, and Oki-Kami Guri Banks (Sakai, 1971; Astakhova and Mel'nichenko, 2002); these locations correspond precisely to the locations where samples with high Ba concentrations were collected. Sakai (1971) proposed that barite nodules were formed by hydrothermal activity during the Quaternary glaciation based on oxygen and sulfur isotopic data, although the barite nodules are found in Miocene–Pliocene siltstone (Hirase Group). Astakhova and Mel'nichenko (2002) proposed that barite precipitated during the interactions of Ba-bearing solutions with sulfates of mud water. These workers pointed out that barite nodule occurrences are spatially inhomogeneous within the Hirase Group. Therefore, the distribution of Ba concentration outliers differs from those of Be and La concentration.

7. Summary

We elucidated the controls of marine sedimentary environments on the spatial distribution of elements using comprehensive geochemical maps of both the land and sea of the Tohoku region, Japan and its surroundings. Particle transportation through large rivers was identified as the dominant factor affecting the distribution of silt and clay on the continental shelf off of Niigata and around Sendai Bay. These areas are particularly abundant in Li, Cu, Zn, As, Mo, Cd, Sn, Sb, Hg, Pb, and Bi. These geochemical features are simply controlled by the grain size effect and do not reflect the geochemistry of the adjacent terrestrial area.

Coarse sands on the continental shelf are relict sediments. These sands contain large amounts of quartz coated with Fe hydroxides, which absorb As dissolved in water effectively. Distributions of Li, Be, P_2O_5, K_2O, Cr, Ni, Rb, Y, Nb, Sb, Cs, Ba, REEs, Ta, Tl, Th, and U are continuous between the Kitakami Mountains and near-shore regions such as offshore from Kamaishi. These relict sediments are inferred to have originated from coastal erosion and/or denudation of basement rocks during past regression and transgression because they are deposited at water depths of 50–150 m where they are unaffected by water action. The sandy sediments that occur widely on the shelf and slope of the Pacific Ocean in this region are homogenous across water depths, which suggests that these sandy sediments on the shelf have been transported by gravity-driven processes to the deep sea and have been influenced little by the denudation of basement rocks.

High concentrations of MgO, Al_2O_3, CaO, Sc, TiO_2, V, MnO, Fe_2O_3, Co, Ga, and Sr in sandy sediments on the continental shelf off of Hachinohe are explained as the result of denudation of Miocene volcanic materials. Sediments enriched in Li, Be, K_2O, Rb, Nb, Cs, Ba, REEs, Ta, Th, and U in submarine topographic highs in the Sea of Japan are attributed to the denudation of Miocene sedimentary rocks associated with acidic tuff and barite nodules.

The marine environment of the Sea of Japan is dominantly hemipelagic and pelagic. Early diagenetic processes enhance the concentrations of MgO, P_2O_5, TiO_2, Cr, MnO, Co, Ni, Cu, As, Mo, Cd, Sn, Sb, Hg, Pb, and Bi in clays deposited in the deep-sea basins under oxic condition associated with the Japan Sea Proper Water. The deep continental slope on the Pacific Ocean side also exists under hemipelagic sedimentary conditions with sediments enriched in Li, Cr, Ni, Cu, Zn, Mo, Cd, Sb, Cs, Hg, Bi, and U.

Therefore, the spatial distribution patterns of elements in these marine sediments are strongly controlled by their depositional environments. However, except for grain size effect and input of local geological materials, the elemental abundance patterns of these marine sediments are comparable between the Pacific Ocean and the Sea of Japan.

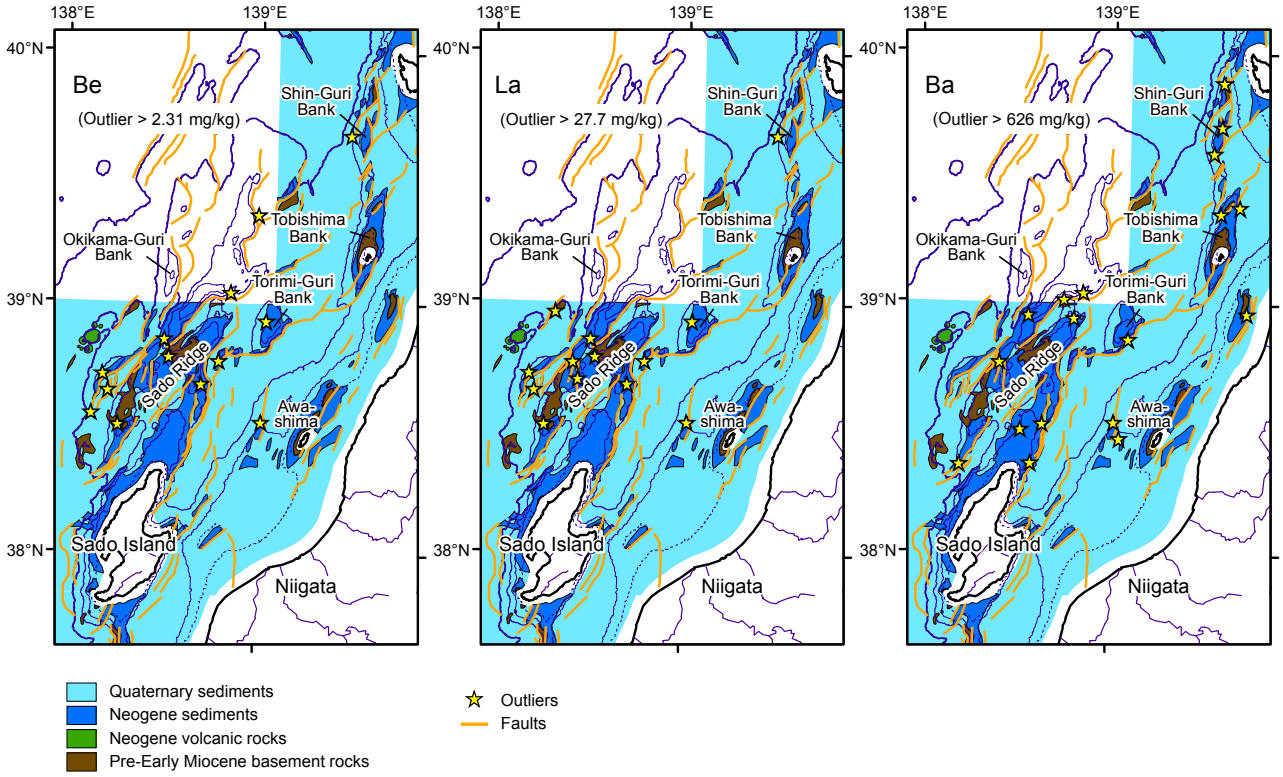

Fig. 9 Distributions of outliers in Be, La and Ba concentrations in marine sediments and marine geological maps at a scale of 1:200,000 (Okamura *et al*., 1994, 1995a, 1996a, b).

Acknowledgements

The authors express their appreciation to Dr. T. Okai (Geological Survey of Japan, AIST) for his useful suggestions, which helped to improve an earlier version of this manuscript. The authors are grateful to the Japan Oceanographic Data Center (JODC) for providing data files.

References

Akimoto, T., Kawagoe, S. and Kazama, S. (2009) Estimation of sediment yield in Japan by using climate projection model. *Proceedings of Hydraulic Engineering*, **53**, 655–660 (in Japanese, with English abstract).

Arita, M. and Kinoshita, Y. (1978) *Sedimentological Map of Offing of Hachinohe*. 1:200,000 Marine Geology Map Series 9, Geological Survey of Japan.

Arita, M. and Kinoshita, Y. (1984) *Sedimentological Map of off Kamaishi*. 1:200,000 Marine Geology Map Series 25, Geological Survey of Japan (in Japanese, with English abstract).

Astakhova, N. and Mel'nichenko, Y. I. (2002) Barite nodules in the Japan Sea. *Lithology and Mineral Resources*, **37**, 39–46.

Fritz, C. O., Morris, P. E. and Richler, J. J. (2012) Effect size estimates: current use, calculations, and interpretation. *J. Exp. Psychol. Gen*., **141**, 2–18.

Gamo, T., Nozaki, Y., Sakai, H., Nakai, T. and Tsubota, H. (1986) Spatial and temporal variations of water characteristics in the Japan Sea bottom layer. *J. Mar. Res*., **44**, 781–793.

Geological Survey of Japan, AIST (ed.). (1992) *Geological Map of Japan, 1:1,000,000 (3rd, ed.)*. Geological Survey of Japan.

Goldich, S. S. (1938) A study in rock-weathering. *J. Geol.*, **46**, 17–58.

Grubbs, F. E. (1969) Procedures for Detecting Outlying Observations in Samples. *Technometrics*, **11**, 1–21.

Honza, E., Tamaki, E. and Murakami, F. (1978) Geological Map of the Japan and Kuril Trenches and the adjacent areas. *1:1,000,000 Marine Geology Map Series 11*.

Howarth, R. J. and Thornton, I. (1983) Regional Geochemical Mapping and its Application to Environmental Studies. *In* Thornton, I., ed., *Applied Environmental Geochemistry*, Academic Press, London, 41–73.

Iijima, A. and Kagami, H. (1961) Cainozoic tectonic developement of the continental slope, northeast of Japan. *J. Geol. Soc. Japan*, **67**, 561–577 (in Japanese, with English abstract).

Ikehara, K., Katayama, H. and Nakajima, T. (1994a) *Sedimentological Map of the Vicinity of Awashima*. 1:200,000 Marine Geology Map Series 42, Geological

Survey of Japan (in Japanese, with English abstract).
Ikehara, K., Nakajima, T. and Katayama, H. (1994b) *Sedimentological Map West of Akita*. 1:200,000 Marine Geology Map Series 41, Geological Survey of Japan (in Japanese, with English abstract).
Imai, N. (1987) Multielement analysis of stream sediment by ICP-AES. *Bunseki Kagaku*, **36**, T41–T45 (in Japanese, with English abstract).
Imai, N. (1990) Multielement analysis of rocks with the use of geological certified reference material by inductively coupled plasma mass spectrometry. *Anal. Sci*., **6**, 389–395.
Imai, N., Terashima, S., Katayama, H., Nakajima, T., Ikehara, K. and Taniguchi, M. (1997) Geochemical behavior of heavy metals in coastal marine sediments from the eastern margin of the Japan Sea. *Bull. Geol. Surv. Japan*, **48**, 511–530 (in Japanese, with English abstract).
Imai, N., Terashima, S., Ohta, A., Mikoshiba, M., Okai, T., Tachibana, Y., Togashi, S., Matsuhisa, Y., Kanai, Y., Kamioka, H. and Taniguchi, M. (2004) *Geochemical map of Japan*. Geological Survey of Japan, AIST, 209p (in Japanese, with English abstract).
Imai, N., Terashima, S., Ohta, A., Mikoshiba, M., Okai, T., Tachibana, Y., Togashi, S., Matsuhisa, Y., Kanai, Y. and Kamioka, H. (2010) *Geochemical Map of Sea and Land of Japan*. Geological Survey of Japan, AIST, Tsukuba, 207p (in Japanese, with English abstract). Database available from https://gbank.gsj.jp/geochemmap/ (accessed 2016-07-12).
Katayama, H., Nakajima, T. and Ikehara, K. (1994) *Sedimentological Map South of Sado Island*. 1:200,000 Marine Geology Map Series 44, Geological Survey of Japan (in Japanese, with English abstract).
Nakajima, T. (1973) Submarine topography off the southern part of Sanriku district. *J. Geogr. (Chigaku Zasshi)*, **82**, 136–147 (in Japanese, with English abstract).
Nakajima, T., Katayama, H. and Ikehara, K. (1995) *Sedimentological Map North of Sado Island*. 1:200,000 Marine Geology Map Series 45, Geological Survey of Japan (in Japanese, with English abstract).
Nishimura, A. and Saito, Y. (2016) *Sedimentological Map off Kinkasan*. 1:200,000 Marine Geology Map Series, no. 87 (CD), Geological Survey of Japan, AIST (in Japanese, with English abstract).
Noda, A. and TuZino, T. (2007) Characteristics of sediments and their dispersal systems along the shelf and slope of an active forearc margin, eastern Hokkaido, northern Japan. *Sediment. Geol*., **201**, 341–364.
Ohta, A. and Imai, N. (2011) Comprehensive Survey of Multi-Elements in Coastal Sea and Stream Sediments in the Island Arc Region of Japan: Mass Transfer from Terrestrial to Marine Environments. *In* El-Amin, M., ed., *Advanced Topics in Mass Transfer*, InTech, Croatia, 373–398.
Ohta, A., Imai, N., Terashima, S., Tachibana, Y., Ikehara, K., Okai, T., Ujiie-Mikoshiba, M. and Kubota, R. (2007) Elemental distribution of coastal sea and stream sediments in the island-arc region of Japan and mass transfer processes from terrestrial to marine environments. *Appl. Geochem*., **22**, 2872–2891.
Ohta, A., Imai, N., Terashima, S., Tachibana, Y., Ikehara, K., Katayama, H. and Noda, A. (2010) Factors controlling regional spatial distribution of 53 elements in coastal sea sediments in northern Japan: Comparison of geochemical data derived from stream and marine sediments. *Appl. Geochem*., **25**, 357–376.
Ohta, A., Imai, N., Terashima, S. and Tachibana, Y. (2011) Regional geochemical mapping in eastern Japan including the nation's capital, Tokyo. *Geochem.-Explor. Environ. Anal*., **11**, 211–223.
Ohta, A., Imai, N., Terashima, S., Tachibana, Y. and Ikehara, K. (2013) Regional spatial distribution of multiple elements in the surface sediments of the eastern Tsushima Strait (southwestern Sea of Japan). *Appl. Geochem*., **37**, 43–56.
Ohta, A., Imai, N., Terashima, S., Tachibana, Y., Ikehara, K. and Katayama, H. (2015) Elemental distribution of surface sediments around Oki Trough including adjacent terrestrial area: Strong impact of Japan Sea Proper Water on silty and clayey sediments. *Bull. Geol. Surv. Japan*, **66**, 81–101.
Okamura, Y. (2010) Relationships between geological structure and earthquake source faults along the eastern margin of the Japan Sea. *J. Geol. Soc. Japan*, **116**, 582–591 (in Japanese, with English abstract).
Okamura, Y. (2013) Active Faults in Japan Sea revealed by topography and geology. *Reports of seismic crusutal and activities in Japan discussed in the 198th, 199th meetings are recorded*., **90**, p. 530–536. The coordinating Commitee for Earthquake Prediction, Japan (in Japanese).
Okamura, Y. and Tanahashi, M. (1983) *Geological Map off Kamaishi*. 1:200,000 Marine Geology Map Series 22, Geological Survey of Japan (in Japanese, with English abstract).
Okamura, Y., Takeuchi, K., Joshima, M. and Satoh, M. (1994) *Geological Map South of Sado Island*. 1:200,000 Marine Geology Map Series 43, Geological Survey of Japan (in Japanese, with English abstract).
Okamura, Y., Takeuchi, K., Joshima, M. and Satoh, M. (1995a) *Geological Map North of Sado Island*. 1:200,000 Marine Geology Map Series 46, Geological Survey of Japan (in Japanese, with English abstract).
Okamura, Y., Watanabe, M., Morijiri, R. and Satoh, M. (1995b) Rifting and basin inversion in the eastern margin of the Japan Sea. *Isl. Arc*., **4**, 166–181.
Okamura, Y., Morijiri, R. and Satoh, M. (1996a) *Geological Map West of Akita*. 1:200,000 Marine Geology Map Series 48, Geological Survey of Japan (in Japanese, with English abstract).
Okamura, Y., Morijiri, R., Tsuchiya, N. and Satoh, M.

(1996b) *Geological Map of the Vicinity of Awashima*. 1:200,000 Marine Geology Map Series 47, Geological Survey of Japan (in Japanese, with English abstract).

Reimann, C. (2005) Geochemical mapping: technique or art? *Geochem.: Explor. Environ. Anal*., **5**, 359–370.

Reimann, C., Siewers, U., Tarvainen, T., Bityukova, L., Eriksson, J., Gilucis, A., Gregorauskiene, V., Lukashev, V., Matinian, N. and Pasieczna, A. (2003) *Agricultural Soils in Northern Europe: A Geochemical Atlas*. E. Schweizerbart'sche Verlagsbuchhandlung, Stuttgart, Germany, 279p.

Richardson, J. T. (2011) Eta squared and partial eta squared as measures of effect size in educational research. *Educational Research Review*, **6**, 135–147.

Saito, Y. (1989) Classification of shelf sediments and their sedimentary facies in the storm-dominated shelf: A review. *J. Geogr. (Chigaku Zasshi)*, **98**, 350–365.

Sakai, H. (1971) Sulfur and oxygen isotopic study of barite concretions from banks in the Japan Sea off the Northeast Honshu, Japan. *Geochem. J*., **5**, 79–93.

Salminen, R., Batista, M. J., Bidovec, M., Demetriades, A., B., D. V., De Vos, W., Duris, M., Gilucis, A., Gregorauskiene, V., Halamic, J., Heitzmann, P., Lima, A., Jordan, G., Klaver, G., Klein, P., Lis, J., Locutura, J., Marsina, K., Mazreku, A., O'Connor, P. J., Olsson, S. Å., Ottesen, R.-T., Petersell, V., Plant, J. A., Reeder, S., Salpeteur, I., Sandström, H., Siewers, U., Steenfelt, A. and Tarvainen, T. (2005) *Geochemical atlas of Europe. Part 1 —Background Information, Methodology and Maps*. Geological Survey of Finland, Espoo, Finland, 526p.

Shaw, T. J., Gieskes, J. M. and Jahnke, R. A. (1990) Early diagenesis in differing depositional environments: The response of transition metals in pore water. *Geochim. Cosmochim. Acta*, **54**, 1233–1246.

Shimamura, K. (2008) Revised chart of the submarine canyon and valley systems around the Japanese Islands —on their topographic features and their unsettled questions. *J. Geol. Soc. Japan*, **114**, 560–576 (in Japanese, with English abstract).

Sullivan, K. A. and Aller, R. C. (1996) Diagenetic cycling of arsenic in Amazon shelf sediments. *Geochim. Cosmochim. Acta*, **60**, 1465–1477.

Tamaki, K. (1978) *Geological Map off Hachinohe*. 1:200,000 Marine Geology Map Series 10, Geological Survey of Japan.

Tamaki, K., Honza, E., Yuasa, M., Nishimura, K. and Murakami, F. (1981) Geological Map of the Central Japan Sea. *1:1,000,000 Marine Geology Map Series 15*.

Taylor, S. R. and McLennan, S. M. (1995) The geochemical evolution of the continental crust. *Rev. Geophys*., **33**, 241–265.

Terashima, S. and Katayama, H. (1993) Geochemical behavior of twelve elements in marine sediments from of Niigata, Japan. *Bull. Geol. Surv. Japan*, **44**, 55–74 (in Japanese, with English abstract).

Terashima, S., Katayama, H., Nakajima, T. and Ikehara, K. (1995a) Geochemical behavior of mercury in coastal marine sediments off Niigata, southeastern margin of the Japan Sea. *Chikyukagaku (Geochemistry)*, **29**, 25–36 (in Japanese, with English abstract).

Terashima, S., Nakajima, T., Katayama, H., Ikehara, K., Imai, N. and Taniguchi, M. (1995b) Geochemical behavior of heavy metals in marine sediments from the off Akita-Yamagata, Japan Sea. *Bull. Geol. Surv. Japan*, **46**, 153–176 (in Japanese, with English abstract).

Ujiie-Mikoshiba, M., Imai, N., Terashima, S., Tachibana, Y. and Okai, T. (2006) Geochemical mapping in northern Honshu, Japan. *Appl. Geochem*., **21**, 492–514.

Weaver, T. A., Broxton, D. E., Bolivar, S. L. and Freeman, S. H. (1983) *The Geochemical Atlas of Alaska: Compiled by the Geochemistry Group, Earth Sciences Division, Los Alamos National Laboratory*. GJBX-32(83), Los Alamos, 141p.

Webb, J. S., Thornton, I., Thompson, M., Howarth, R. J. and Lowenstein, P. L. (1978) *The Wolfson Geochemical Atlas of England and Wales*. Clarendon Press, Oxford, 69p.

Yashima, K., Imai, K. and Nishizawa, K. (1982) 1:1,000,000 Bathymetric Charts "Hokkaido", "North-east Nippon" and Submarine Topography. *Report of Hydrographic and Oceanographic Researches*, **17**, 93–162 (in Japanese, with English abstract).

Recieved July 12, 2016
Accepted December 21, 2016

東北地方の多元素海域地球化学図に対し太平洋側と日本海側で堆積環境の違いが与える影響

太田充恒・今井　登・立花好子・池原　研・片山　肇・中嶋　健

要　旨

著者らは東北地方の陸海域包括地球化学図を作成し，海域の堆積環境が広域元素濃度分布にどのような影響を与えるかについて調べた．日本海の堆積物はカリウム，バリウム，希土類元素など珪長質火成岩に多く含まれる元素に富み，特に海底地形の高まりで採取された堆積物に著しく濃集する傾向が認められた．この堆積物は，デイサイト質火山灰やバライト団塊などを伴う新第三紀堆積岩の削剥生成物と考えられる．深海盆に分布するシルトや粘土は，マンガン，カドミウム，鉛などに富んでおり，初期続成作用がこれらの元素の濃集の原因と考えられる．大陸棚のシルト質堆積物は大規模河川から供給されたにもかかわらず，その化学組成は隣接する陸域物質の影響よりは，粒径効果の影響が強く現れていた．太平洋側に広く分布する砂質堆積物は主に，波浪限界深度よりも深い海域で採取された．これらの化学組成は均質であり，苦鉄質火山岩の影響を受けた河川堆積物の化学組成と類似していた．この結果から，これらの堆積物は第四紀の苦鉄質火山活動の影響下で形成された残存堆積物であり，陸棚から深海へ重力流によって移動していったと考えられる．陸域の土砂生産量の内，81%は日本海側へ供給されるが，必ずしも陸と海との間で元素濃度の空間分布に連続性が認められる訳ではない．同様の結果は太平洋側にも認められる．例外的に，釜石沖の粗粒砂は，隣接する陸域に露出する付加帯堆積岩や花崗岩に多く含まれる元素に富む特徴を示す．この地域の河川は皆小規模であることから土砂生産量は少ないことを考慮すると，これらの粗粒砂は海進・海退期に母岩の海岸浸食・削剥などによって形成されたと考えられる．